

**Block copolymer based nanocomposite
membranes for Arsenic and Selenium
removal from coal-fired powerplant
wastewater**



By

Syed Qamber Ali Zaidi

School of Chemical and Materials Engineering

National University of Sciences and Technology

2023

**Block copolymer based nanocomposite
membranes for Arsenic and Selenium
removal from coal-fired powerplant
wastewater**



Name: Syed Qamber Ali Zaidi

Registration No: 00000328787

**This thesis is submitted as a partial fulfillment of the requirements
for the degree of**

MS in Chemical Engineering

Supervisor Name: Dr. Zaib Jahan

School of Chemical and Materials Engineering (SCME)

National University of Science and Technology (NUST)

H-12, Islamabad, Pakistan

July, 2023



THESIS ACCEPTANCE CERTIFICATE

Certified that final copy of MS thesis written by **Syed Qamber Ali Zaidi** (Registration No 00000328787), of School of Chemical & Materials Engineering (SCME) has been vetted by undersigned, found complete in all respects as per NUST Statues/Regulations, is free of plagiarism, errors, and mistakes and is accepted as partial fulfillment for award of MS degree. It is further certified that necessary amendments as pointed out by GEC members of the scholar have also been incorporated in the said thesis.


Signature: 

Name of Supervisor: **Dr. Zaib Jahan**

Date: 07/07/2023

Signature (HOD): 

Date: 18/7/23

Signature (Dean/Principal): 

Date: 11.7.23



National University of Sciences & Technology (NUST)
MASTER'S THESIS WORK
Formulation of Guidance and Examination Committee (GEC)

Form TH-1
(Must be type written)

E/Penal

Name: Syed Qamber Ali Zaidi
 Department: Chemical Engineering (SCME)
 Credit Hour Completed: (18) 24
Course Work Completed

NUST Reg No: 328787
 Specialization: Chemical Engineering
 CGPA: (3.58) 3.69

S/No	Code	Title	Core/Elective	CH	Grade
1	EME 921	Momentum Heat and Mass Transfer	Core	03	A
2	CHE 843	Separation Processes in Chemical Engineering	Core	03	B+
3	ENE 809	Wastewater Treatment and Design	Elective	03	A
4	RM 898	Research Methodology	Elective	02	Q
5	CHE-847	Chemical Kinetics & reactor design	Core	03	B
6	CHE-816	Molecular Nanotechnology	Elective	03	B+
7	EME-981	Advanced Fuel Technology	Elective	03	B+

Date: 13-09-2021

Student's Signature: *Qamber*

Thesis Committee

- Name: Dr. Zaib Jahan (Supervisor)
Department: School of Chemical & Materials Engineering
- Name: Dr. Faheem Hassan Akhtar
Department: Department of Chemistry and Chemical Engineering LUMS (Co-supervisor)
- Name: Dr. Nasir Muhammad Ahmad
Department: School of Chemical & Materials Engineering
- Name: Dr. Ali Inam
Department: IESE

Signature: *Zaib Jahan*
 Signature: *Faheem*
 Signature: *Nasir*
 Signature: *Ali Inam*

Date: 20/9/21

Signature of Head of Department: *EB*

APPROVAL

Date: 20.9.2021

Signature of Dean/Principal: *AB*

Distribution

- 1x copy to Exam Branch, Main Office NUST
 1x copy to PGP Die, Main Office NUST
 1x copy to Exam branch, respective institute

School of Chemical and Materials Engineering (SCME) Sector H-12, Islamabad

- * 8. ESE-911 Carbon capture & Utilization Elective 03 A
 9. CHE-015 Nanocatalysis Elective 03 A



National University of Sciences & Technology (NUST)

FORM TH-4

MASTER'S THESIS WORK

We hereby recommend that the dissertation prepared under our supervision by

Regn No & Name: 0000328787 Syed Qamber Ali Zaidi

Title: Block Copolymer Based Nanocomposite Membranes for Arsenic and Selenium Removal from Coal-Fired Powerplant Wastewater.

Presented on: 08 Jun 2023 at: 1430 hrs in SCME Seminar Hall

Be accepted in partial fulfillment of the requirements for the award of Master of Science degree in Chemical Engineering.

Guidance & Examination Committee Members

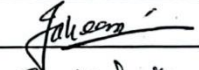
Name: Dr Nasir M Ahmad

Signature: 


Name: Dr Ali Inam (IESE)

Signature: 

Name: Dr Faheem Hassan Akhtar (Co-Supervisor)

Signature: 

Supervisor's Name: Dr Zaib Jahan

Signature: 

Dated: 05/7/2023


Head of Department
Date 01/7/23


Dean/Principal
Date 07-07-23

School of Chemical & Materials Engineering (SCME)

Dedication

By the grace of Almighty Allah, who is the most Beneficent and
the most merciful

This research is dedicated to my parents, who have always been
my source of guidance and support.

To my supervisor who shared his knowledge, gave advice, and
encouraged me to fulfill my tasks.

And to all my fellows, with whom I worked with and shared good
memories.

Acknowledgements

All praises to Almighty Allah, without His will nothing can happen, who favored us with the capacity to think and made us anxious to investigate this entire universe. Incalculable greetings upon the Holy Prophet Hazrat Muhammad (PBUH), the reason for the creation of the universe and wellspring of information and blessing for whole humankind.

From the core of my heart, I am thankful to my research supervisor, Dr. Zaib Jahan for her unwavering technical and moral support and enlightening me with a research vision and pushing me for excellence. Her quest for perfection and excellence had been a source of inspiration and driving force. It is her consistent and encouragement that empowered me to achieve this onerous milestone.

I extend my sincere gratitude towards my guidance and committee members: Dr. Faheem Hasan Akhtar, Dr. Nasir Muhammad Ahmad, and Dr. Muhammad Ali Inam for guiding and supporting me in my research course. It would not have been possible without them. I express my utmost gratitude to Dr. Muhammad Bilal Khan Niazi and Dr. Sulalit Bandyopadhyay for their efforts in enabling me to get Erasmus Global Mobility Scholarship to NTNU Norway.

I am thankful of My Seniors who shared their knowledge regarding experimental techniques, and they motivated me in this entire research work. Without any doubt, SCME's supporting staff coordinated with me while I was working on different equipment.

I am highly obligated to my Parents and siblings for their never-ending love. Thanks for believing in me, wanting the best for me, and inspiring me to follow my passion. To my friends, particularly Hizbullah, Mashal, and Arslan, thank you for your support, advice, and encouragement.

Syed Qamber Ali Zaidi

Abstract

The severity of risks caused by arsenic and selenium ions in aqueous environments are well-known. Novel thin film block copolymer based nanocomposite membranes are synthesized for an efficient removal of these toxic ions. Nexar, a commercially available amphiphilic sulfonated pentablock copolymer creates a self-ordering and a long range nano morphology. The resultant morphologies thus creating nano-highways helps in improving the flux through the resultant membranes. The effect of fouling in the membranes are countered by using octaphenyl-POSS as the nanofiller. The second phase of work aims at surface modification of Polyether imide nanofiltration membranes with enhanced separation for arsenic and selenium. Specifically, a zwitterionic copolymer comprising MPC and AEMA is synthesized via a one-pot free-radical polymerization. Different amounts of MPC and AEMA monomers were introduced at molar ratios of 5:5, 7:3, and 9:1 to tune the physicochemical properties of the newly developed copolymer and the effect on the filtration performance of these varied molar ratios of the monomers is kept under check. Comparative analysis was done based on results obtained from both works. Membranes modified with zwitterionic materials imparted their hydrophilic properties to the membranes with the WCA as low as 22° were observed for copolymers with molar ratio 7:3(MPC: AEMA). Whereas for the Nexar membranes with POSS incorporated the WCA were not as low. Based on the rejections, the membranes were also compared with the copolymeric membranes modified with water and TEA showing superior results than its counterpart as well as those with POSS incorporated Nexar membranes with rejection of 99.49% and 98.78% for arsenic and selenium respectively.

Table of Contents

Dedication	i
Acknowledgements	ii
Abstract	iii
List of Figures	vii
List of Tables	xi
Acronym	xii
Chapter 1	1
Introduction	1
1.1 Background.....	1
1.2 Problem Statement	3
1.3 Research Objectives	3
1.4 Scope of Study.....	4
1.5 Chapter Summary	4
Chapter 2	6
Literature Review	6
2.1 Polymer	6
2.1.1 Background	6
2.1.2 Polymer synthesis.....	7
2.1.3 Step Growth Polymerization	8
2.1.4 Chain or Addition Polymerization	9
2.1.5 Free Radical Polymerization	10
2.1.6 Copolymer	10
2.1.7 Types of Copolymers	11
2.1.8 Copolymerization	12
2.2 Membrane	14

2.2.1 Background	14
2.2.2 Classification	15
2.2.3 Materials	18
2.2.4 Membrane Synthesis	19
2.2.5 Membrane Fouling	21
2.2.6 Membrane Modification: Antifouling	22
2.3 Wastewater Treatment	23
2.3.1 Arsenic	23
2.3.2 Selenium	24
2.3.3 Removal of Arsenic and Selenium	24
Chapter 3	26
Materials and Methods	26
3.1 Materials	26
3.1.1 Nexar Membranes	26
3.1.2 P[MPC-co-AEMA]	26
3.1.3 PEI-m- P[MPC-co-AEMA] Membranes	26
3.2 Methods	26
3.2.1 Nexar Membranes synthesis	26
3.2.2 P[MPC-co-AEMA] synthesis	27
3.2.3 PEI-m- P[MPC-co-AEMA] Membranes synthesis	28
3.3 Characterization Techniques	29
3.3.1 Fourier Transform Infrared Spectroscopy (ATR-FTIR)	29
3.3.2 Nuclear Magnetic Resonance (NMR)	30
3.3.3 Thermogravimetric Analysis (TGA)	31
3.3.4 Scanning Electron Microscopy (SEM)	32
3.3.5 Atomic Force Microscopy (AFM)	33
3.3.6 Drop Shape Analyzer (DSA)	34

3.3.7 Water Uptake.....	35
3.4 Dead-end Filtration	35
3.4.1 Pure Water Permeability (PWP).....	36
3.4.2 Arsenic and Selenium Rejection	37
Chapter 4.....	38
Results and discussion.....	38
4.1 Polymer characterization	38
4.1.1 Fourier Transform Infrared Spectroscopy	38
4.1.2 Nuclear Magnetic Resonance	39
4.1.3 Thermogravimetric Analysis	40
4.2 Membrane Characterization.....	41
4.2.1 Fourier Transform Infrared Spectroscopy	41
4.2.2 Scanning Electron Microscopy	44
4.2.3 Atomic Force Microscopy.....	46
4.2.4 Water Contact Angle	50
4.2.5 Water Uptake.....	53
4.3 Membrane Testing	54
4.3.1 Pure Water Permeability	54
4.3.2 Arsenic and Selenium Rejections.....	56
Conclusion	58
Future Recommendations	59
References:.....	60

List of Figures

Figure 1: Polymer classification	6
Figure 2: Step-growth polymerization schematic	8
Figure 3: Addition polymerization schematic.....	9
Figure 4: Types of copolymers	11
Figure 5: Homopolymerization and Copolymerization	13
Figure 6: Membrane Separation Mechanism	14
Figure 7: Membrane Classification	16
Figure 8: Membrane size Regimes	18
Figure 9: Membrane Fouling Mechanisms	22
Figure 10: Synthesis scheme of Nexar membranes	27
Figure 11: P[MPC-co-AEMA] synthesis scheme.....	28
Figure 12: Synthesis scheme PEI-m-P[MPC-co-AEMA] membranes.....	29
Figure 13: Working mechanism of ATR-FTIR	30
Figure 14: Working Mechanism of NMR.....	31
Figure 15: Working Mechanism of TGA.....	32
Figure 16: Working Principle of SEM.....	33
Figure 17: Working Principle of AFM	34
Figure 18: Working mechanism of DSA	35
Figure 19: Working of Dead-end Filtration process	36
Figure 20: FTIR spectra of the P[MPC-co-AEMA] copolymer and monomers	38

Figure 21: FTIR spectra of the P[MPC-co-AEMA] copolymer with different molar ratios.....	39
Figure 22: Proton nuclear magnetic resonance (¹ H NMR) spectra of (a) MPC (b) AEMA (c) P[MPC-co-AEMA].....	40
Figure 23: TGA curves of the P[MPC-co-AEMA] copolymer with different molar ratios.....	41
Figure 24: FTIR Spectra of Nexar membranes with THF as solvent	42
Figure 25: FTIR Spectra of Nexar membranes with IPA and Toulene as solvent.....	42
Figure 26: FTIR spectra PEI-m-P[MPC-co-AEMA] membranes with water and TEA.	43
Figure 27: FTIR spectra PEI-m-P[MPC-co-AEMA] membranes with water and IPA ..	44
Figure 28: SEM images of (i) Nexar membranes with IPA and Toluene as solvent (a) Top Section (b) Cross-section (c) EDX analysis (ii) 0.5wt% POSS incorporated Nexar membranes with IPA and Toluene as solvents (a) Top Section (b) Cross-section (c) EDX analysis	45
Figure 29: Cross sectional SEM images of (a) Pure PEI (b) PEI-m-P[MPC-co-AEMA](7:3) with water and TEA (c) PEI-m-P[MPC-co-AEMA](7:3) with water and IPA	46
Figure 30: AFM images of (a) Pure Nexar (b) 0.5wt% POSS (c) 5wt% POSS with THF as solvent.....	47
Figure 31: AFM images of (a) Pure Nexar (b) 0.5wt% POSS (c) 5wt% POSS with IPA and Toulene as solvent.....	47

Figure 32: Figure 31: AFM images of (a) Pure PEI (b) PEI-m-P[MPC-co-AEMA] (5:5) with water and TEA (c) PEI-m-P[MPC-co-AEMA] (7:3) with water and TEA (d) PEI-m-P[MPC-co-AEMA] (9:1) with water and TEA	48
Figure 33: AFM Images of (a) Pure PEI (b) PEI-m-P[MPC-co-AEMA] (5:5) with water and IPA (c) PEI-m-P[MPC-co-AEMA] (7:3) with water and IPA (d) PEI-m-P[MPC-co-AEMA] (9:1) with water and IPA	49
Figure 34: Water Contact Angles of Nexar membranes with THF as solvent	50
Figure 35: Water Contact Angles of Nexar membranes with IPA+Toluene as solvent .	51
Figure 36: Water Contact Angles of PEI-m-P[MPC-co-AEMA] membranes with water+TEA.....	52
Figure 37: Water Contact Angles of PEI-m-P[MPC-co-AEMA] membranes with water+IPA	52
Figure 38: Water Uptake for Nexar membranes with THF and IPA+Toluene as solvents	53
Figure 39: Water Uptake for PEI-m-P[MPC-co-AEMA] with water+TEA and water+IPA	54
Figure 40: Pure Water Permeability for Nexar membranes with THF and IPA+Toluene as solvents	55
Figure 41: Pure Water Permeability for PEI-m-P[MPC-co-AEMA] with water+TEA and water+IPA	56
Figure 42: Arsenic and Selenium rejections for Nexar membranes with (a)THF (b) IPA+Toluene as solvents	57

Figure 43: Arsenic and Selenium rejections for PEI-m-P[MPC-co-AEMA] with(a)

Water+TEA (b) Water+IPA..... 57

List of Tables

Table 1: Copolymer Characteristics.....	12
Table 2: Surface roughness parameters determined by AFM for Nexar membranes with THF as solvent	47
Table 3: Surface roughness parameters determined by AFM for Nexar membranes with THF and IPA+Toluene as solvents	48
Table 4: Surface roughness parameters determined by AFM for PEI-m-P[MPC-co-AEMA] with Water and IPA	49
Table 5: Surface roughness parameters determined by AFM for PEI-m-P[MPC-co-AEMA] with Water and TEA.....	49

Acronym

NF Nanofiltration

BCP Block copolymer

SEM Scanning Electron Microscope

FTIR Fourier Transmission Infrared Spectroscopy

TGA Thermogravimetric Analysis

NMR Nuclear Magnetic Resonance

DSA Drop Shape Analyzer

Chapter 1

Introduction

1.1 Background

Groundwater is considered a major source of drinking water in the majority of underdeveloped countries. The toxicity of heavy metals such as arsenic, mercury, selenium etc. in waterbodies has been identified as a global challenge[1]. With increasingly stringent regulations on wastewater discharge, various industries are demanding efficient methods to remove these toxins. The sources of these heavy metals in environment can be natural as well as anthropogenic[2]. The industrial wastewater, if discharged untreated into the water bodies, consist of high levels of heavy metals concentration which can be responsible for environmental pollution as well as toxic for humans. Organic contaminants tend to biodegrade, which is not the case with heavy metals as they can accumulate into living organisms causing a number of toxic diseases which ranges from acute to chronic. Hence, the development of treatment technologies for the removal of such inorganic heavy metals which are also cost-effective in nature is pivotal moving forward into the future[3].

The usage of polymers are used extensively nowadays in a various field and are deemed significantly important, to meet market demands in each field. This shift of high consumption broadened by the usage of such materials which ranges from industrial to modern technology markets such as: optics, nanoscience and biomedical has created a room for an in-depth study in polymer sciences.

In this regard, membrane separation processes such as electrodialysis (ED), reverse osmosis (RO) and nanofiltration (NF) have been employed as heavy metal removal processes ranging from laboratory scale to industrial level[4]. Membrane separation performance is evaluated on selectivity as well as the permeance in terms of flux. Such optimization can be hampered by problems such as fouling in the membranes which

reduces the process efficiency as well as the lifetime of the membranes. Modern polymer studies are focused upon addressing this issue and providing solutions to such complications encountered in wastewater treatment processes from membrane technology.

Currently, there exist a lot of interest in studying the membrane modifications done in terms of antifouling. Addition of hydrophilic materials into polymers are studied and analyzed for increased hydrophilicity. This in turn aids in the formation of hydration surrounding the membrane surfaces needed to avoid unwanted foulants adhesion. PEG is a frequently used hydrophilic agent. The ability of forming water bonds and charge neutrality through hydrogen bonding makes it a potential candidate to improve hydrophilicity. The downside is that PEG is easy to oxidize and therefore, maintaining the hydrophilicity in long-term filtration is a challenge associated with its usage. Surface hydrophilicity can have modification via functionalization with nanomaterials having hydrophilic properties. These can include silica nanoparticles, POSS particles, graphene oxide, carbon nanotubes etc.[5].

In this work, initially Polyhedral oligomeric silsesquioxane (POSS) nanoparticles were incorporated in the Nexar nanofiltration membranes for the concurrent removal of arsenic and selenium from wastewater. The choice of POSS as the nanoparticle owes to the fact these nanoparticles have:

- Antifouling properties
- high functionalization flexibility
- Smaller size range (1-10nm)
- High dispersion and compatibility when incorporated in diverse polymer matrices at the molecular level[6].

Herein, we synthesized POSS incorporated in sulfonated pentablock copolymer Nexar membranes. The influences of POSS chemistry in terms of loading in the polymer matrix was investigated based upon the rejection and permeability. We aim to develop an effective nanocomposite membrane comprising of POSS and Nexar. This work aims to concurrently remove arsenic and selenium from the aqueous solutions. So far, there has

been limited work done in the field of block copolymers based membranes for the heavy metal removal. This study promises to design better nanofiltration membranes for mining industry wastewater, particularly the wet flue gas desulfurization streams toxic ions removal.

Zwitterionic polymeric materials have found considerable interest in this field and been used for membrane modification as a new class of antifouling agents. Such zwitterionic polymers tend to possess both functional groups having both positive and negative charges. Such properties have caused an extensive and widespread research interest of studying these strong hydrophilic zwitterions[7].

Keeping all these aspects into consideration, the second phase of the research work is based upon synthesis of a zwitterionic copolymer. The copolymer is intended to increase the antifouling and anti-scaling properties of a polyetherimide membrane. The surface modification of the membrane is done via reacting/coating the copolymer onto the polymeric membranes. Lastly, heavy metals rejections are also tested for these copolymers modified membranes.

1.2 Problem Statement

- Coal-fired powerplants produced wastewater composing of heavy metals in concentration of higher values.
- Arsenic and selenium present in the wastewater is responsible for causing several diseases.
- In this regard, membrane based separation has been studied to separate arsenic and selenium from the wastewater.

1.3 Research Objectives

To overcome the existing challenges in heavy metals wastewater, the following objectives were identified.

- Look out for possible alternatives of existing antifouling materials used in the

membrane synthesis for wastewater treatment.

- Synthesis of such antifouling materials as well as their incorporation in the polymeric membranes was also under studied.
- Finally, the comparative analysis of the results based on the results given by antifouling membranes was done.

1.4 Scope of Study

The following scope was established to ensure that the research would be carried out in the time available

- Rejections of arsenic and selenium from the synthesized polymeric membranes was considered as the scope of this research.
- The membranes were characterized using analytical techniques and subjected to dead end filtration to test them for heavy metals separation.
- Based on the results obtained after the rejection studies, membranes with higher efficiencies were compared with the studies done before.

1.5 Chapter Summary

The thesis has been mainly designed in the following way

- **Chapter 1:** In the first chapter discusses the theoretical aspects of polymer synthesis based studies.
- **Chapter 2:** It also focuses on the membranes for heavy metal removal in chapter 2 and focuses upon the relevance of the work from the literature and the aim is to let the reader make aware of the changing trends in water treatment processes.
- **Chapter 3:** Chapter 3 discusses the methodology of synthesis of copolymer and membrane synthesis. The characterization techniques used in synthesis of both polymers and membranes are also discussed.
- **Chapter 4:** In Chapter 4, all the outcomes and results of the characterization of copolymer synthesis and membranes. At the end the conclusion of this research and

future guidelines of research are presented.

- **Chapter 5:** Conclusions and future recommendations of the research are presented in the last part of the thesis.

Chapter 2

Literature Review

2.1 Polymer

2.1.1 Background

The word polymer comes from Greek origin word poly and term meros, means many parts[4]. Polymers represents a class of materials made up of chainlike and large molecules. These larger molecules are comprised of smaller molecules which are termed as monomers. Building blocks of polymers are monomers and join to form the polymers. There can be as many monomer molecules as possible in one polymer molecule and the more they are the stronger the polymer chain. The arrangement of these repeating units allows various types of chains that can be synthesized, and these chains are shaped in a way to bend themselves. Consequently, a class of materials that are characterized by an intriguing range of properties are thus formed named as polymeric materials[8].

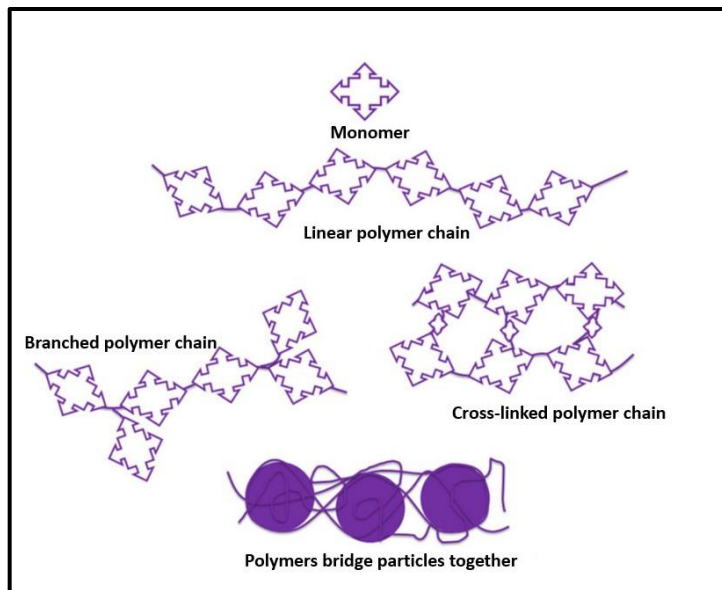


Figure 1: Polymer classification [9]

There are monomers present which contains charges both negative and positive separately as well as combined and these form their structure by assembling in a chain-like configuration. Based on charge of the monomers, a polymer is categorized into cationic, anionic, nonionic, and amphoteric. These charged monomers can determine the overall charge density of the polymers quantitatively in percentage amounts. On the basis the chain orientation, the classification of the polymers can be done as linear, branched, and cross-linked[9].

2.1.2 Polymer synthesis

The chain morphologies can be determined based upon the polymerization reactions. These reactions are started through monomer molecules addition on propagating center which are active. This addition is done through the new bond formations which resultantly forms a macromolecule having high molecular weight. Polymerization is a general process having multistep hence the non-uniform chain length in each polymer exists. The degree of polymerization normally is in correspondence to the monomer units amount present in a macromolecule. There are several polymerization mechanisms e.g., ionic —anionic polymerization, radical polymerization, living anionic polymerization, cationic polymerization, ring-opening polymerization, multimode polymerization, and coordination polymerization[9]. Main methods of polymerization among these all mechanism of polymerization mostly in industrial use are ionic (both cationic and anionic), radical and coordination polymerization. Polymerization such as living radical polymerization and ring-opening polymerization are relatively new and known to be promising methods for obtaining novel products. It is convenient to categorize the polymerization reactions into two or three basic types. These are condensation and addition polymerization and most of the polymerization fit easily into these two categories apart from some exceptions. In condensation polymerization reaction the chemical repeat unit of the polymer has a different molecular formula to that of the monomer constituting it. A typical condensation polymerization is the formation of ester from ethyl alcohol and acetic acid where the water molecule is eliminated giving it a name condensation.

In contrast, the structural unit of the addition polymers have the same molecular formula as their monomers. A typical example of such addition polymerization is synthesis of polyethylene from ethylene having the same repeating units in the product as the monomer constituting the polymer possesses. However, there are some polymerization reactions that do not fit easily into these categories. Synthesis of polyurethanes from isocyanates and alcohols is a condensation polymerization without having water molecule eliminated from the product. Similarly, some ring opening polymerization reactions are regarded as the addition polymerization forms product that can also be produced via condensation polymerization. Accordingly, there has been a classification of polymerization given as it is either considered to be either step-growth (includes polycondensation) or addition/chain polymerization[10].

2.1.3 Step Growth Polymerization

The characteristic feature of such a polymerization is the slow buildup of a chain. The systematic fashion of such a step wise growth is shown in the figure. Combination of the monomers give dimers and trimers followed by oligomers and so on. This eventually provides a molecular weight polymer of higher number after the polymerization. Several important polymers such as nylon(polyamides), polycarbonates, polyurethane etc. are produced through such polymerizations[11, 12].

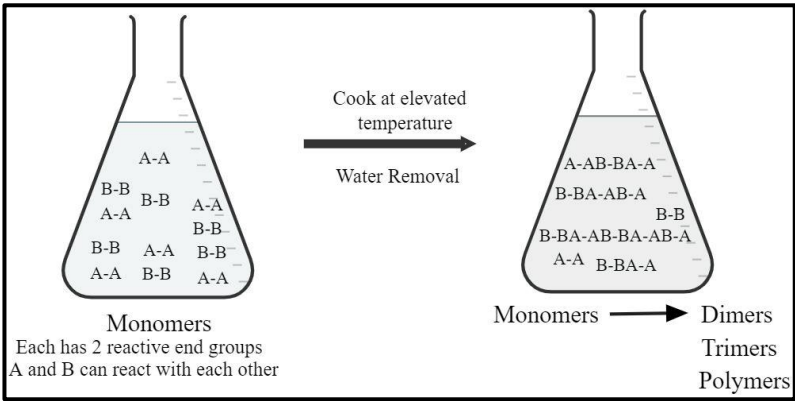


Figure 2: Step-growth polymerization schematic

2.1.4 Chain or Addition Polymerization

Addition or chain polymerization is a mechanism where an active site is present at the end of a growing chain where the monomers are added in a sequential manner. In such a polymerization, only a few species are active. At any instant of time of species distribution, the system as shown in figure is mainly consisting upon the

- (a) fully formed polymer chains having no reactive sites
- (b) monomer which are unreacted
- (c) small growing chains

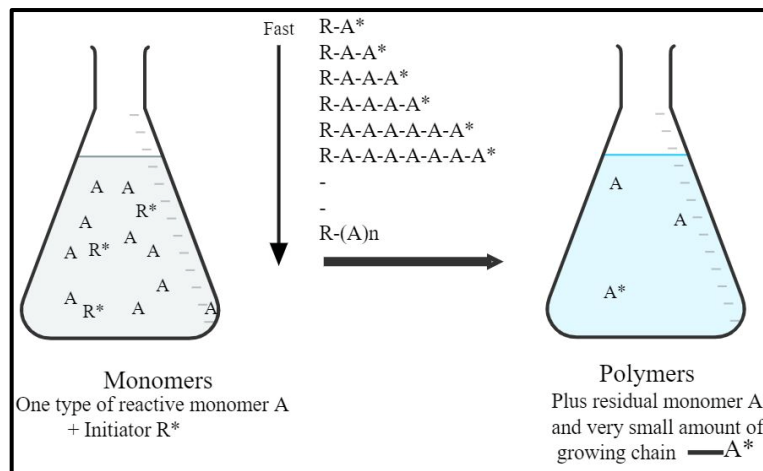


Figure 3: Addition polymerization schematic

The formation of active sites in such polymerization can have several forms which allows a range of polymer and copolymer synthesis. In general, addition polymerization have the following common features:

- (i) There is an initiation of the polymerization by means of which active sites are generated on monomers.
- (ii) The chain propagation happens by the monomers addition on the active site of the propagating chain and the active site simultaneously being transferred to the newly added monomer.
- (iii) Termination of the polymerization due to the destruction of the active site[13].

2.1.5 Free Radical Polymerization

The key factors of addition polymerization can be discussed by focusing attention on an important type named free radical polymerization. Historically it is said that an impurity (peroxide) in benzaldehyde played a role in performing a reaction which was not intended and gave rise to free radical polymerizations. These species are termed as initiators as they give rise to initiate the polymerization by breaking down to give radicals. The mechanism of these radical initiated polymerization is in correspondence to the above mentioned process for the addition polymerization. The free radicals provide the initiation followed by the propagation of the growing chains which proceeds rapidly. The termination of the reaction occur when the two radical meet in the process of random collisions[12, 14].

2.1.6 Copolymer

There is often a desire of modification the properties of a homopolymer. This is particularly done with the purpose of certain application-specific characteristics which a homopolymer alone perhaps cannot possess. There could well be an interest in achieving properties that are present in the two homopolymers. Generally, crystallinity, flexibility, melting point, glass transition temperature, tensile strength etc. are the properties of interest considered and aimed for copolymers. Blending one homopolymer with another is one option which would end up in a physical mixture. This is done through mechanical methods namely extrusion and screw compounding. One issue with blending is that there exists a phase separation tendency and is not as straightforward as it looks. This is due to the inherent incompatibility which exists between most of the polymers.

One way to counter this issue is the introduction of functionalities of specific interactive nature such as hydrogen bonding and ion–dipole interactions on the homopolymer pairs. It is roughly estimated that 36 percent of worldwide consumption of polymers are blended polymeric products. An alternative of such a process is referred to as copolymerization which is the polymerization of two or more monomers and the polymer is named as a copolymer. In case when more than two monomers are added, the copolymer is termed as multicomponent copolymer and the term terpolymer is for the special case with three monomers. Addition of the monomers of different types to the reaction mixture results in

enhanced properties but also brings in added kinetic reaction mechanisms complexities. Such complexities are because of relative rates of polymerization which are dependent upon the monomer structure and radicals as well. These multicomponent systems thus can influence the composition of the polymer, sequence of the monomers, and molecular weight of the polymer. Copolymers brings applications which have broader ranges and homopolymers have limited applications in such fields.

2.1.7 Types of Copolymers

Classification of the copolymers can be done since the arrangements of the monomers of two or more types in the chain or their monomer distribution can allow them to be categorized. Four types of copolymers are classified for linear cases: random, alternating, block, and gradient copolymers[15].

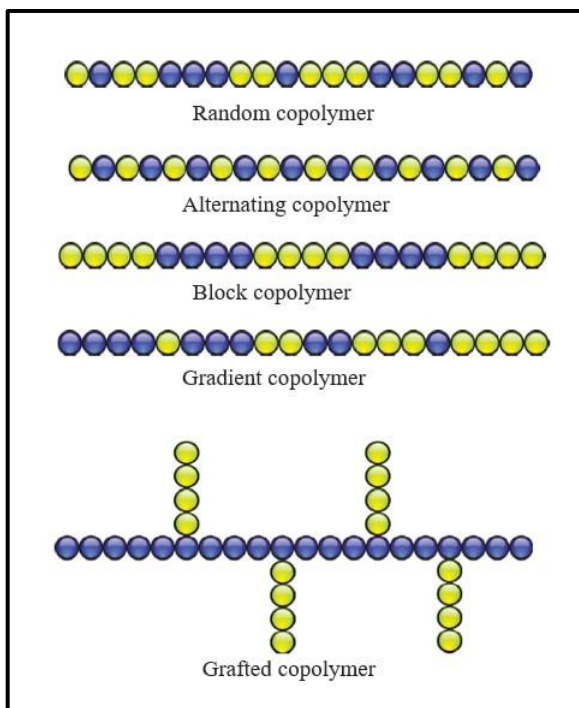


Figure 4: Types of copolymers

Table 1: Copolymer Characteristics

Copolymer	Characteristics
Statistical Copolymers/Random Copolymers	Statistical copolymers are characterized by their monomer sequence which follows a statistical law (Markovian statistics).
Alternating Copolymers	Alternating copolymers follows an alternating pattern and composed of the monomers which are in equimolar composition.
Block Copolymers	Block copolymers are specified by the monomer sequences with at least one long monomers sequence of each monomer should be present.
Gradient Copolymers	Gradient copolymers have an initial chain portion of rich in one monomer unit with its concentration gradually decreasing across the chain length, while second monomer has its concentration increased across the chain length.
Graft Copolymers	Graft copolymers are characterized by the branched chains that are formed of a main homopolymer chain of one monomer and branches of homopolymer of a second monomer that can be single or several.

2.1.8 Copolymerization

Initially, copolymers have been defined as the species containing more than one type of monomers/chemical units in the same chain. Based upon their arrangements of these units in the chain, they have been categorized into different types as well.

The synthesis of these copolymers are based upon the same types of chemistry as previously discussed in the polymer synthesis section. Chain growth polymerization can be used to synthesized statistical or random copolymers via addition of two monomers A and B in the reaction vessel. The denotation of active site by a *overleaf on either of these monomers could be a radical, ionic species or a coordination complex.

Distribution of such species in the chains depends upon the rate at which one monomer adds to the growing chain relative to the other. Such statistical distribution because of this is possible to be described in terms of their ratio constants or reactivity ratios.

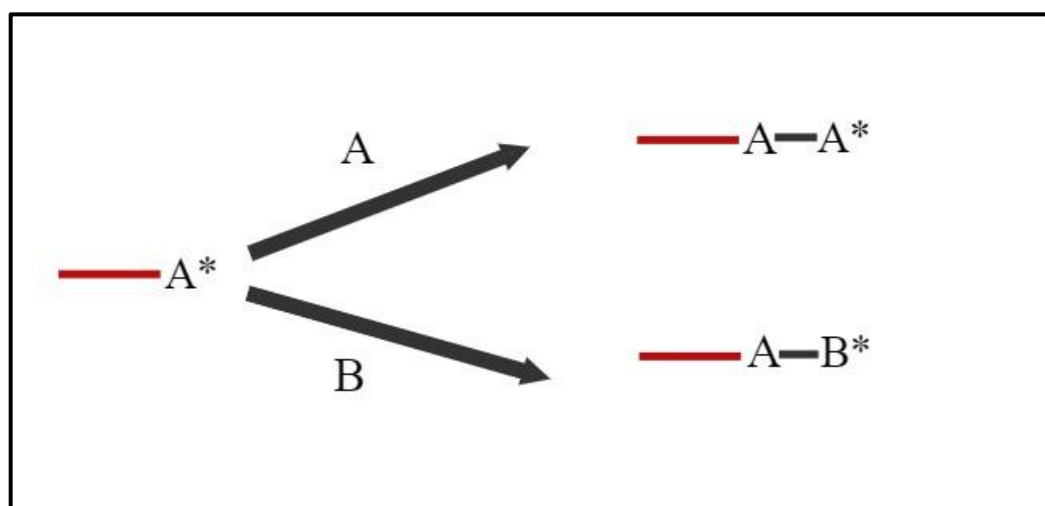


Figure 5: Homopolymerization and Copolymerization

Other types of copolymers have slight variation for the copolymerization such as a block copolymer can be synthesized firstly by polymerizing short polymer chains called as macromers with single functional group (acid) at each end and another macromer polymerized by a distinct as well as a complementary functional group at its ends. These individual macromers can then be reacted to form long chains. An example from the automobile industry is the usage of thermoplastic elastomers which are synthesized in a similar manner.

The kinetics of chain growth polymerization particularly free radical are focused and will be studied extensively showing the knowledge of kinetics which allows the prediction of the instantaneous composition of the copolymers[12]

2.2 Membrane

2.2.1 Background

Systematic studies done for the membrane phenomena has been done for centuries by now and can be taken back to the 18th century. In this regard, Abb'e Nolet was the first in line as he introduced the term 'osmosis' which described the water permeation phenomena through a diaphragm in 1748. Initially, membranes were limited to lab usage and did not have any industrial or commercial uses throughout the nineteenth and early twentieth century.

The period from 1960-1980 changed the membrane technology altogether. It was structured upon building on the original technique of Loeb-Sourirajan. Different membrane techniques such as multilayer composites, interfacial polymerizations and coatings were also formally originated for synthesizing high performance and efficient membranes. Thus, membranes comprising of selective layer of thickness 0.1 μ m or less are now being produced for various applications. Until 1980, most of the of the membrane separation processes such as microfiltration, ultrafiltration, nanofiltration, reverse osmosis and electro dialysis were matured with their industrial applications[16].

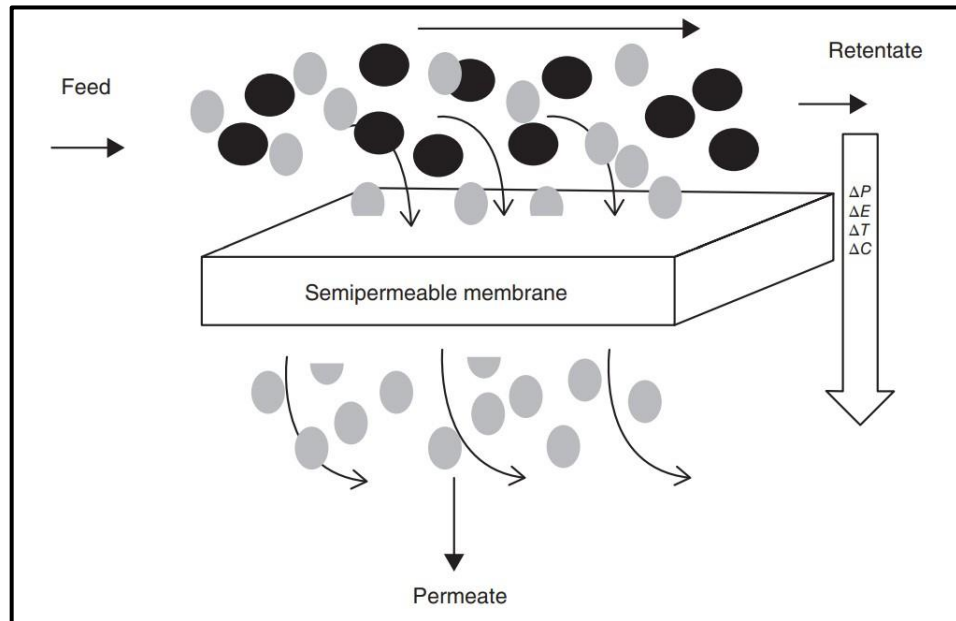


Figure 6: Membrane Separation Mechanism [17]

Membrane technology is mainly differentiated from traditional separation and purification as it can produce stable products without adding chemicals.

In addition, this is done with a relatively low energy consumption which also contributes to the environment in a greener way. Other advantages of membrane technology includes well-arranged, ease of scale up, modular nature, compactness, and straightforward process. All these benefits in operation decreases the operation as well as capital cost of technologies that use membrane applications[17].

2.2.2 Classification

Classification of the membranes depending on the origin, nature, morphology, method is shown in figure. Main classes of synthetic membranes are categorized as: organic (polymer) and inorganic. Inorganic membranes are typically ceramics and zeolites based, such as alumina, titania, and zirconia. The membranes are constituted of high mechanical and chemical stability, and elevated temperature and pressure resistance in comparison to organic membranes. However, these are also high cost membranes, which restricts their industrial application. Whereas polymeric synthetic membranes are the class of membranes having an extensive variety of structures and properties.

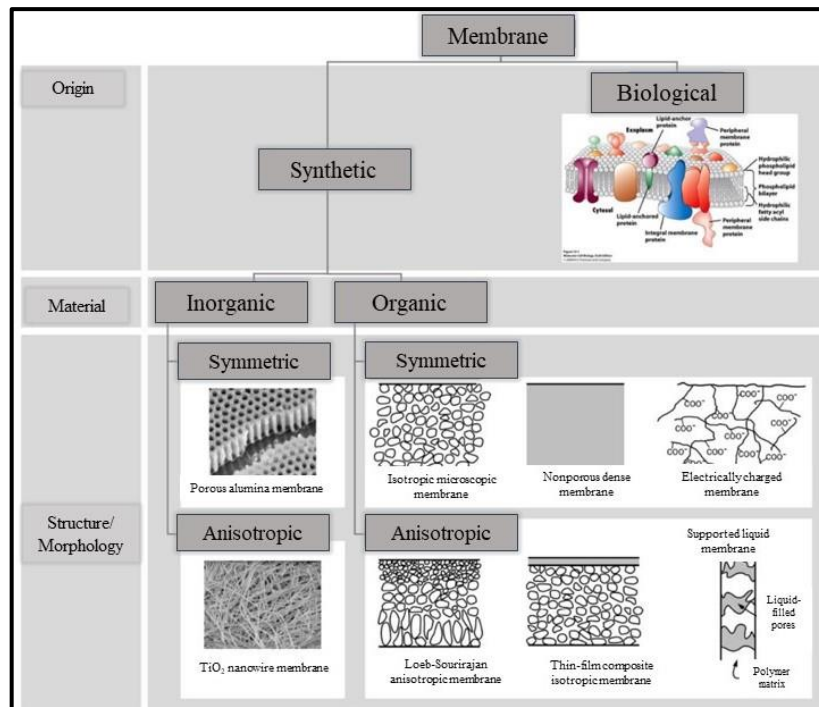


Figure 7: Membrane Classification [16]

Considering the morphology and structure of the membrane, they can either be homogenous having uniformity in composition and structure or can be possessing layered structure or pores making it heterogeneous. Moreover, further classification can be made based on the symmetry of membranes which can be either symmetrical (isotropic) or anisotropic. In this regard, microporous, electrochemically charged, and dense membranes can be divided among the isotropic membranes. Anisotropic membranes can be categorized into integrally asymmetric, supported liquid membranes, and composite.

Classification of the membranes based on the size regimes employs several types which is based upon the size of pores: reverse osmosis, nanofiltration, ultrafiltration, microfiltration, and particle filtration. MF membranes are characterized for their larger pore sizes which ranges from 0.1–5 μm and typically reject particles of size ranging in this size range such as bacteria, asbestos, and red blood cells. UF membranes comprises of smaller pores than MF membranes ranging in between 0.01–0.1 μm and is able in filtering out large particle, microorganisms, dissolved bio-macromolecules. Nanofiltration membranes are also porous membranes and filter particles in range of 0.001–0.01 μm and

exhibits filtering that lies between UF and RO. Most organic molecules, viruses, multivalent salts can be filtered out using nanofiltration membranes. Since nanofiltration membranes are able to reject divalent ions, they are also used to soften hard water. RO membranes are considered as dense membranes as the pores are considered as nonporous with size ranging from approx. 0.0001–0.001 μm .

These size ranges include thermal motion of the polymer which are responsible for forming membranes. Thus, reverse osmosis membranes have the capability of filtering out species having lower molecular weights which includes inorganic solids such as monovalent ions, metallic ions and organic molecules[18]

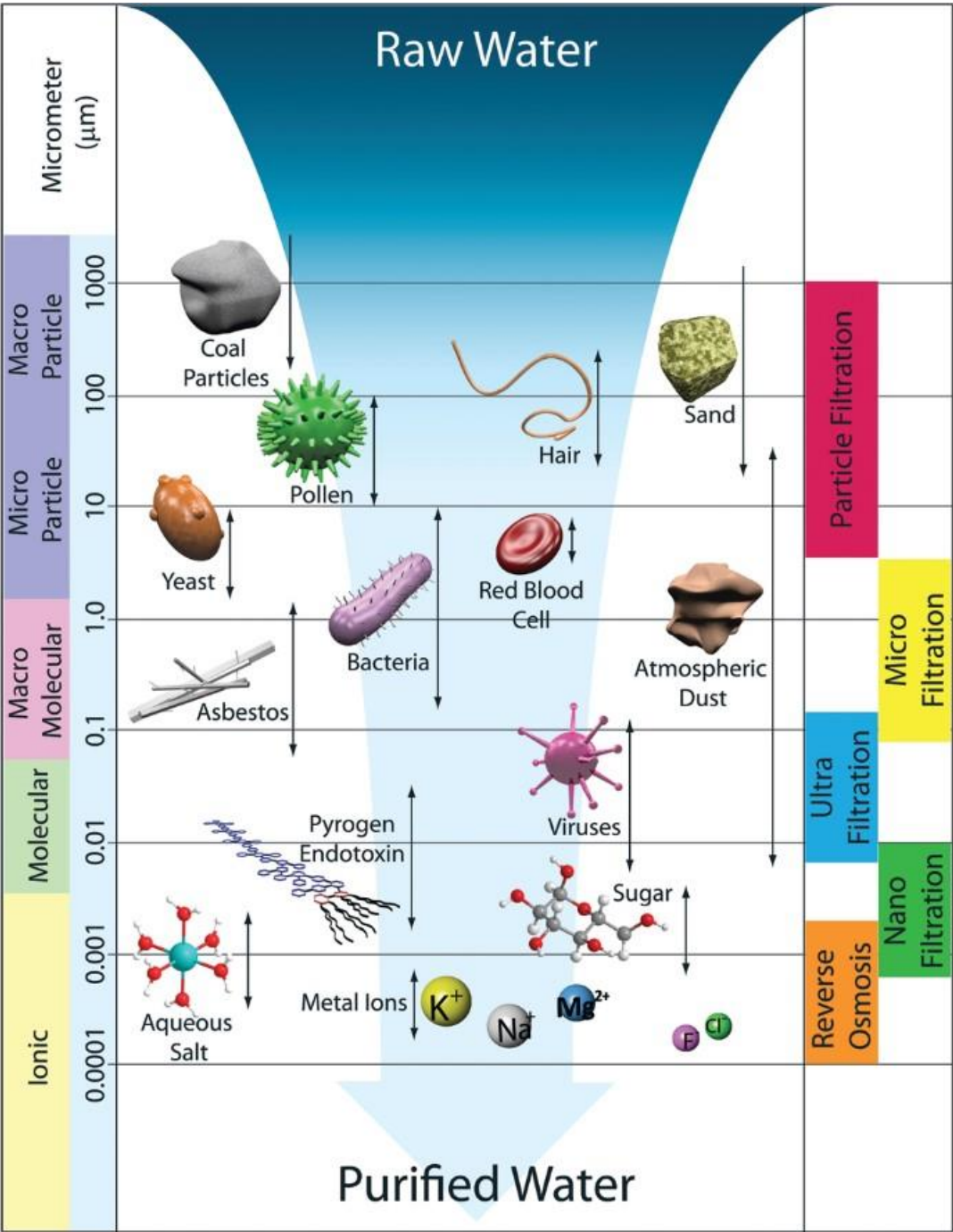


Figure 8: Membrane size Regimes [18]

2.2.3 Materials

The choice of membrane materials for an effective membrane design depends upon various factor which includes high solute rejection and water flux, physiochemical

stability, system design, module configuration, and operating conditions for cost-effectiveness. Governing factors for the membrane performance are the porous structure and the physicochemical properties of material. An extensive amount of work has been done in exploring new membrane materials as well as potential ways to modify the materials used in the recent past. NF, UF, and MF used in water treatment synthetic polymers (polyacrylonitrile, polyvinylidene fluoride, polysulfide, and polyacrylonitrile)-polyvinyl chloride) copolymers. Therefore, only organic-polymeric membranes will be discussed[16, 19].

Organic Materials for Heavy metal removal

Polymers are generally preferred for membrane separation technologies because of their ease of operation. They are also cheaper as compared to inorganic membranes since they use metals, oxides, and ceramics. Active layer and porous support of the membrane can be synthesized using polymers in reverse osmosis, nanofiltration, ultrafiltration, microfiltration processes. In addition to this, there are certain limitations and challenges in the use of polymers for filtration, such as the hydrophobicity issues and membrane fouling. A wide range of polymers have been used to address such issues including polyamide, cellulose acetate, polyvinyl chloride, polyimide, polysulfone, polyvinyl alcohol, polyethersulfone, polyvinylidene fluoride, polyethylene glycol (PEG), poly(methacrylic acid) (PMAA)[20, 21]. In the recent past, extensive work has also been done in the use of block copolymers having self-assemblies. This class of polymers have narrow pore-size distribution which offers high selectivity, high permeability is also resulting from high membrane porosity. These membranes have controllable dimensions, enhanced surface properties, and chemistries. Most of the recent studies done to improve water flux, salt rejection and antifouling properties of membranes and nanocomposites are achieved through a technique named surface modification. Such a techniques involve the usage of zwitterionic coatings, graphene oxide and carbon nanotubes as nanofillers[9].

2.2.4 Membrane Synthesis

Several fabrication methods of membranes are available such as solution casting, interfacial polymerization, phase inversion, sputtering, extruding, melt pressing etc. For

the fabrication of polymeric membranes, phase inversion, solution casting, stretching, track-etching, interfacial polymerization and electrospinning are generally used. The selection of such a technique for a particular membrane is dependent upon the various factors including efficiency of the membrane, cost of synthesis and the desired properties. Membrane performance and morphology are a thermodynamic function, whereas thermodynamics of a membrane is dependent upon selectivity and pressure difference that is applied across the membrane. Thereby, increasing thermodynamic efficiency increases the permeation as well as selectivity of membrane. The membrane synthesis methods used for the research work is discussed in detail as follows.

Solution Casting

The membrane fabrication done through solution casting method is done by preparing the homogenous solution. This is done through polymer dissolution and additives in some common solvent. This can either be done by simply casting a solution prepared in a petri dish of desired shape. Another way to do is spreading prepared polymer solution on a leveled flat plate with the help of a casting knife. The precise slit of a desired thickness can be achieved using a casting knife. The resultant cast solution is then left for the solvent evaporation. This forms a thin polymer film through solution casting. The solvents which are used for the preparation of polymer solution are moderately volatile such as acetone or cyclohexane. Such volatile solvent allows obtaining a dry film of membranes after subjecting them through different drying methods based upon the end properties needed. In case of large durations solvent evaporation, the casted membrane film absorbs moisture which results in polymer precipitation and opaque surface of the polymer film are formed. On the contrary, rapid evaporation leads to the polymer gelation that leads to a mottled surface[22].

Phase Inversion

Phase separation is known to be the most frequently used membrane fabrication method for isotropic and anisotropic polymeric membranes. In principle, the basis of this technique is upon homogeneous polymer solution precipitation into polymer- and solvent-rich phases. The phase rich in polymer is the solid phase, which is responsible for the

membrane matrix, solvent-rich phase which is the polymer-lean phase is responsible for pore formation within the membrane matrix. The precipitation of the polymer solution in the phase separation can be achieved by various methods. Therefore, phase separation method can be distinguished into following types

1. Nonsolvent-Induced phase separation referred to as Loeb–Sourirajan process, where the initial polymer solution precipitation is caused by immersing into some nonsolvent bath which is mostly water.
2. Temperature-Induced Phase Separation, where the precipitation of polymer solution is done by cooling casting solution.
3. Evaporation-Induced Phase Separation, where the precipitation is achieved evaporating the solvent which is volatile from the cast polymer solution.
4. Vapor-Induced Phase Separation (VIPS), where precipitation of the polymer solution is done through the nonsolvent adsorption from the vapor phase[23].

2.2.5 Membrane Fouling

Membrane fouling is defined as the deposition of solute or some other species in the feed system onto the membrane surface or within the pores of the membrane. The gel layer which is formed causes a mass transfer resistance in addition to that provided by the membrane itself. Increment in the transmembrane pressure in such cases further densifies the gel layers. Membrane fouling can be because of pore geometry/tortuosity or wall interactions between pore and species. As a result of this, the pores of the membranes are blocked entirely or marginally. This resultantly causes a decline in transmembrane flux. Different types of membrane fouling are shown in Figure 9 which explains that fouling is dependent upon operating parameters such as feed concentration and also time dependent.[24].

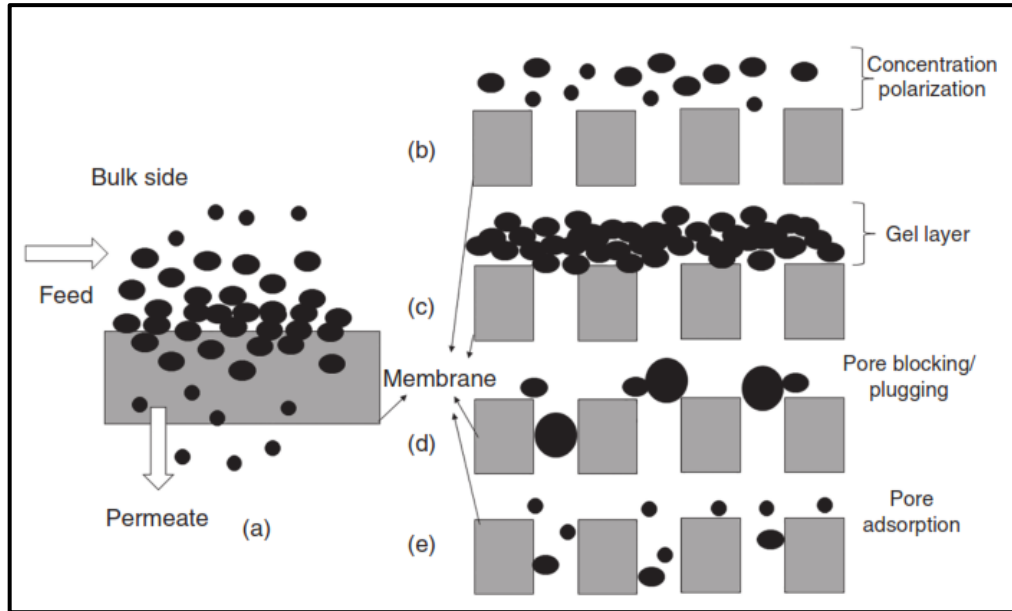


Figure 9: Membrane Fouling Mechanisms [17]

2.2.6 Membrane Modification: Antifouling

The interaction of the wastewater water comprising of foulants with the membrane surfaces leads to scaling of these foulants on the membrane surfaces and this phenomenon of membrane fouling degrades the membrane performance.

The incorporation of hydrophilic and antifouling materials such as PEG and silica- derived nanoparticles to achieve modification of the membrane surface or the bulk structure has resulted in improvement of the performance of filtration processes. This enhancement in the membrane antifouling is done by forming a hydration layer over the membrane surface. This layer enables to form an energetic barrier between the membrane surface and the foulants. However, the property of the hydration layer formed by these antifouling materials are determined by the physio-chemical properties[5].

Among them, the most used hydrophilic material is poly (ethylene glycol) (PEG) based on account of its charge neutrality and ability to form water bonds that it forms via hydrogen bonding. The downside of using PEG is that it is easily oxidized and cannot maintain its hydrophilicity for long-term filtration. In addition, surface hydrophilicity of the nanofiltration membranes can also improve by functionalizing them with hydrophilic

materials such as, carbon nanotubes, graphene oxides, and silica nanoparticles. However, apart from the excellent results, one main challenge is to incorporate these materials into the polymer matrices and keep a check on the agglomeration of these nanomaterials.

To overcome such complications, zwitterions consisting of pendant phosphobetaine, carboxylbetaine, and sulfobetaine groups, give strong surface chemistry. These hydrophilic materials, compared to others consist of both positively and negatively charged groups which allows a stronger and durable hydration layer formation due to electrostatic interactions. Therefore, benefitting from these strengths of durability and ease of functionalization, these zwitterionic materials are used to modify the membrane surfaces to improve their performances especially in terms of their water flux enhancement and improved fouling resistance[7].

2.3 Wastewater Treatment

2.3.1 Arsenic

Arsenic is present in four oxidation states in the environment and is ubiquitously present in it. The four states of Arsenic are arsenate (+5), arsenite (+3), arsenic elemental (0) and arsine (-3)[25]. It is currently ranked 20th in abundance and is widely distributed across the earth's crust. The wide usage of Arsenic is in agricultural fields where it is used as wood preservatives and pesticides. The adverse health effects caused by arsenic includes primarily cancer in humans. Presently huge populations worldwide, especially in the third-world countries, suffer from arsenic poisoning which is mainly caused due to consumption of water and food products with arsenic contamination. Toxicity of different arsenic species can be different such as arsenite (+3) is more toxic than arsenate (+5). Similarly inorganic arsenic species are considered more harmful than organic arsenic species. Such as organic dimethylarsinic acid (DMAV) and monomethylarsonic acid (MMAV) are less toxic from the inorganic but certain intermediates monomethylarsonous acid (MMAIII) and dimethylarsinous acid (DMAIII) are considered more toxic giving us a trend of toxicities as $AsV < MMAV < DMAV < AsIII < MMAIII < DMAIII$ [26, 27].

2.3.2 Selenium

Selenium on the other hand is a metalloid in group VIA and exists in four oxidation states as selenite (+6), selenite (+4), selenium elemental (0) and selenide (-2). Selenium differs from arsenic in a manner that it is considered as an essential nutrient for all living organisms[28]. It is a major component of certain selenium based enzymes and proteins performing essential biological functions therefore, it is vital for certain cellular processes. However, the toxicity of selenium happens above homeostatic requirements and the trend of toxicity is quite like that of arsenic with $SeVI < SeIV$. The major anthropogenic activity which are associated with the selenium mobilization in the environment is coal combustion to produce electric power. Previous studies have reported that selenium has the highest enrichment factor in coal and is the highest among the trace elements. Hence, the potential of selenium enrichment in industrial wastewater is compounded because the natural mineral concentrating processes of Se has been done during waste formation. This makes sustainable bioremediation of selenium a necessity in the global context [26].

2.3.3 Removal of Arsenic and Selenium

Numerous separation technologies have been applied to remove As and Se from wastewater streams. these includes ion exchange, coagulation/precipitation, adsorption, oxidation/reduction and nanofiltration membranes. In this regard, based upon the sustainability principles, nanofiltration membranes from biodegradable polymers have been studied for the removal of heavy metals from wastewater.

Several studies have been done to synthesize novel nanofiltration membranes for arsenic and selenium removal. Andrade et al. studied a nanofiltration treatment route having two nanofiltration stages and an intermediate precipitation stage for the removal of arsenic. Aguiar et al. worked with the simultaneous removal of As and se using combined NF and RO operating system. The feed for the treatment was from gold mine drainage and was treated with the commercial NF99 and RO membranes (HR98PP)[29].

Yingran He et al. is the first reported work to concurrently remove arsenic and selenium using silica based nanoparticles Polyhedral Oligomeric Silsesquioxane (POSS)–Polyamide by incorporating them in polymer membranes to thin-film

nanocomposite nanofiltration membranes will removal efficiency of As and Se above 90% [6].

He et al. was able to synthesize Zr based MOF particles UiO-66, and fabricated thin-film nanocomposite membranes to remove arsenic and selenium with a flux of 11.5 LMH/bar and a rejections of 96% [1].

He et al. also successfully synthesized a hydrophilic zwitterionic co-polymer, P[MPC-co-AEMA], and fabricated novel thin-film composite membranes for arsenic and selenium removal with a PWP of 8.5 LMH/bar and a rejections were higher than 98% [30].

He et al. also studied sodium ion modified carbon quantum dot (Na-CQD) which were incorporated into thin-film nanocomposite membranes for arsenic and selenium removal and reported rejections of 97.5%, 98.2% and 99.5% toward SeO_3^{2-} , SeO_4^{2-} and HAsO_4^{2-} respectively [31].

Muhammad Hamad Zeeshan et al. used PA-CSBF4 membrane (40 mg C-S BF content) with impressive regeneration performance and reported an optimized membrane with 99 % and 98 % rejection of arsenic(III) and selenium ion [32].

Chapter 3

Materials and Methods

3.1 Materials

3.1.1 Nexar Membranes

Commercially available sulfonated pentablock copolymer (Nexar™ MD9200) was acquired by Kraton Polymers (Houston, TX). The Ion Exchange Capacity (IEC) of the polymer is 2.0 meq/g. Solvents used in the fabrication of membranes are tetrahydrofuran, toluene and isopropanol obtained from Sigma Aldrich™. Octaphenyl-POSS nanoparticles were delivered by Macklin.

3.1.2 P[MPC-co-AEMA]

For the synthesis of P[MPC-co-AEMA], DMSO > 99%, MPC 97 %, AEMA, the radical initiator, AIBN was also obtained from Sigma Aldrich. Dialysis tubing MWCO2000 was also purchased from the VWR.

3.1.3 PEI-m- P[MPC-co-AEMA] Membranes

Firstly, for the synthesis of pristine PEI membranes, PEI (MWCO: 35,000 Da), DMAC, PVP were acquired from Sigma Aldrich. Modification of the pristine membranes was done by using the above synthesized P[MPC-co-AEMA]. TEA and IPA to be used along with MQ water respectively as a reaction medium were purchased from Sigma Aldrich.

3.2 Methods

3.2.1 Nexar Membranes synthesis

The morphology of the membranes is highly affected by the choice of solvents when thin films are cast from the polymer solutions. In this work, membrane films are obtained by casting from two different solvent or solvent mixtures. Briefly we synthesize the membranes using 2wt% polymer solution in different solvents. Firstly, THF was used to dissolve the polymer and in the second case a solvent mixture having 85% toluene and 15% IPA was used. For nanocomposite membranes, different loadings of POSS

nanoparticles were incorporated into the polymer solution using priming technique. The loadings of 0.2wt%, 0.5wt%, 1wt%, 3wt% and 5wt% were incorporated and nanocomposite films were prepared.

To avoid macro-phase separation a slow evaporation rate was ensured, and this was done by covering the petri dishes with glass pans or beakers. The resultant films after the slow evaporation were subjected to vacuum drying for 24 hr and 20-30 μ m thick films were prepared[33].

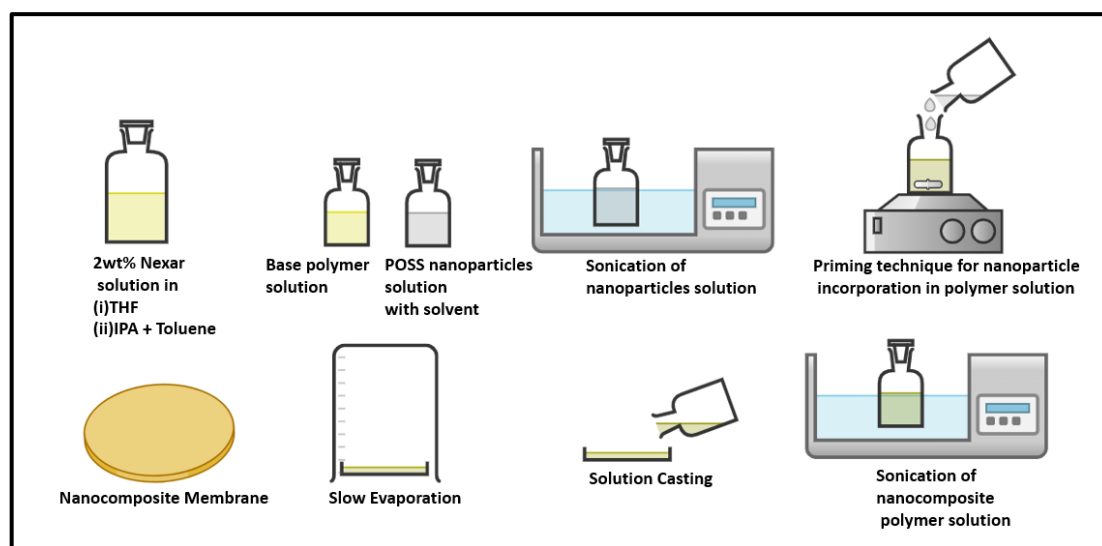


Figure 10: Synthesis scheme of Nexar membranes

3.2.2 P[MPC-co-AEMA] synthesis

Synthesis of P[MPC-co-AEMA], was done through single-step one-pot free-radical polymerization using AIBN as the initiator. In a typical reaction, calculated amounts of AEMA and MPC were introduced into a two-neck round-bottomed flask containing 15 ml MQ water and DMSO solution at a volume ratio of 2/1 and stirred and the mixture was allowed to be purged with nitrogen for 1 h to remove the dissolved oxygen in the reaction system. This was followed by the addition of AIBN initiator and 24h of stirring in a nitrogen atmosphere at 70°C. The purification of copolymerization mixture was done by directly dialyzing the mixture using dialysis tubing (MWCO2000) for 2 days, with the pure water changed twice daily. The dialyzed purified mixture was then freeze-dried to obtain the P[MPC-co-AEMA] white copolymer powder[34].

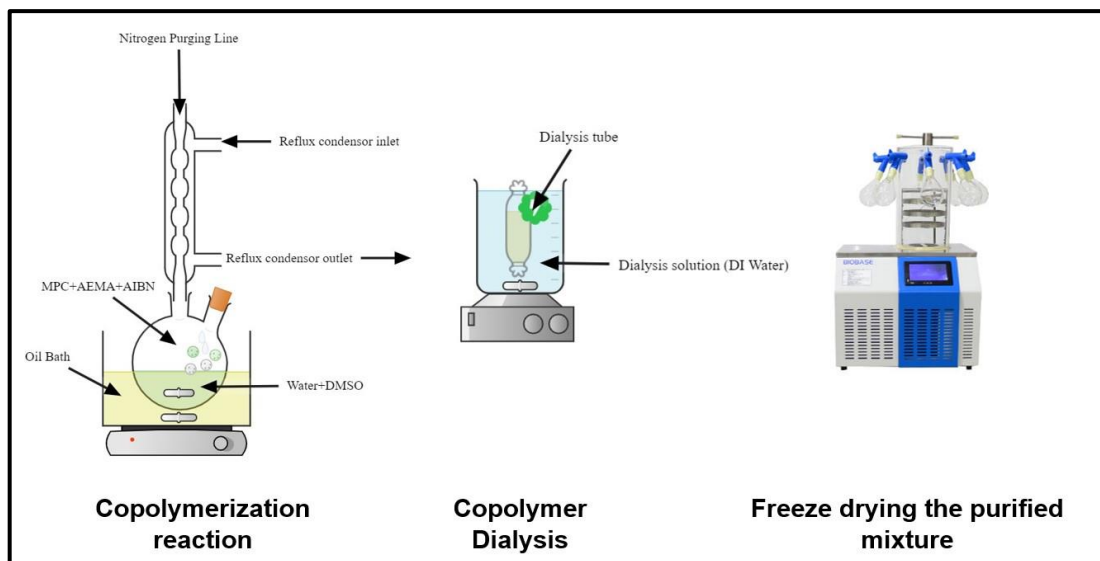


Figure 11: P[MPC-co-AEMA] synthesis scheme

Different amounts of MPC and AEMA monomers were introduced at molar ratios of 5:5, 7:3, and 9:1 to tune the physicochemical properties of the P[MPC-co-AEMA] copolymer. These are denoted as MPC:AEMA-5:5, MPC:AEMA-7:3, and MPC:AEMA-9:1 respectively [35].

3.2.3 PEI-m- P[MPC-co-AEMA] Membranes synthesis

Pristine PEI membranes were prepared by preparing 18 wt% solution in DMAC. Moreover, 2wt % PVP was chosen as a pore former. This was followed by preparing the casting solution by stirring it for 18 h at 60 °C to get a homogeneous solution. To remove the air trapped bubbles the solution was left 12 h without stirring at room temperature. The membranes with the thickness of 120 μm were prepared by spreading the polymer solution on glass plate and casting by a membrane applicator apparatus. The glass plate was then immediately immersed in DI water. To achieve complete phase inversion, membranes were allowed to be soaked into the DI water bath for 24 h [36, 37].

The surface of PEI membranes were modified by grafting the synthesized P[MPC-co-AEMA] zwitterionic copolymer as follows. A 2wt % coating solution was prepared by dissolving the copolymer in 9:1 (wt%) mixture of IPA and water, which was used as one reaction medium [34]. 0.25wt% TEA as a catalyst with water used as a second reaction

medium. Predetermined molar ratios as mentioned above were used to prepare 2wt% solution and the PEI membrane (2.5in diameter) was sealed from both ends and placed inside a reaction solution[7].

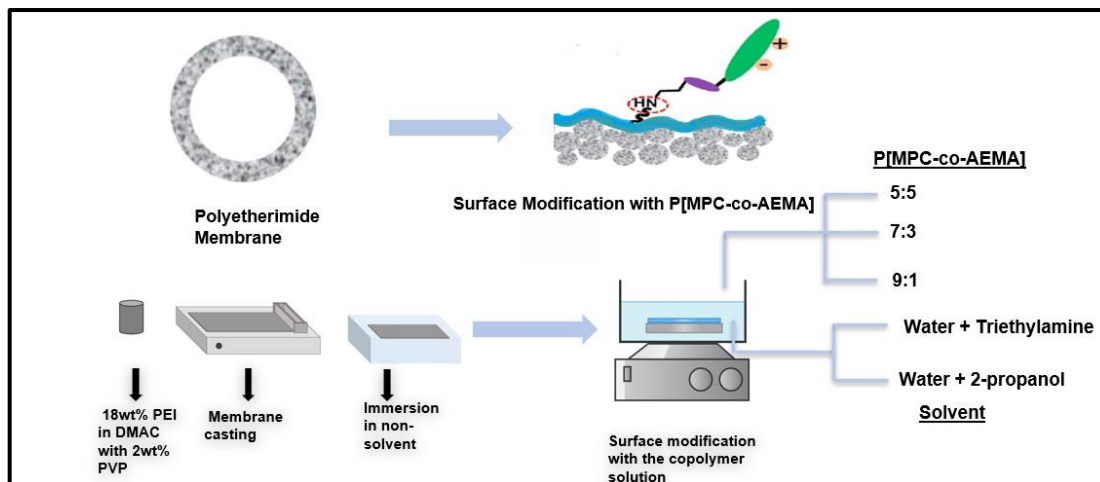


Figure 12: Synthesis scheme PEI-m-P[MPC-co-AEMA] membranes

3.3 Characterization Techniques

3.3.1 Fourier Transform Infrared Spectroscopy (ATR-FTIR)

FTIR analysis was done to specify the functional groups, and interfacial interactions through Attenuated Total reflectance, FTIR (ATR-FTIR, BRUKER Vex 70). The main objectives of FTIR is to determine the characteristic functional groups from each monomer imparting its properties to the copolymer. The range for analysis was 4000-500 cm^{-1} with scanning frequency of 100 and resolution at 4 cm^{-1} . The FTIR analysis of the membranes were also done to determine the changes in terms of the chemical functionalities.

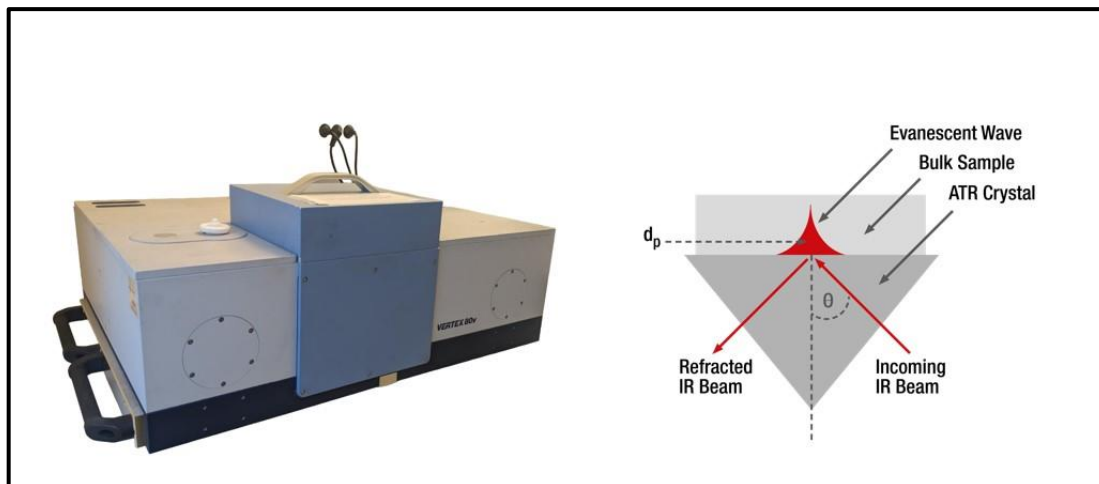


Figure 13: Working mechanism of ATR-FTIR

The working principle of ATR-FTIR spectrometer can be explained where the infrared light passes through a crystal, and this totally internally reflected at crystal-sample interface. This reflected beam goes to the FTIR detector. At the time of internal reflectance, this IR light partially also goes to the sample, and it absorbs it. This wave is referred to as the evanescent wave. Penetration depth for this wave into the sample is calculated by the difference between the ATR crystal and sample refractive index. For different types of samples, different ATR sensors are used of different materials[38].

3.3.2 Nuclear Magnetic Resonance (NMR)

Nuclear Magnetic resonance (NMR) is another spectroscopic technique which is based on the spinning nucleus that gives rise to a magnetic field. The nuclei sample is placed in the magnetic field which is then excited to nuclear magnetic resonance by the use of radio waves. In NMR 600Mhz Bruker Avance, signal is generated because of this which is detected with radio frequency receiver. Intermolecular magnetic field surrounds an atom which varies the resonance frequency. This can provide the structural and compositional details of the molecules. Since the chemical environment of each molecule is different, the resonance frequencies of them will also be different. This allows to have the unique NMR spectra of different molecules. A few of the features which NMR can be used for is to characterize stereoisomerism, sequence- and structural isomerism and look at the copolymer composition[39].

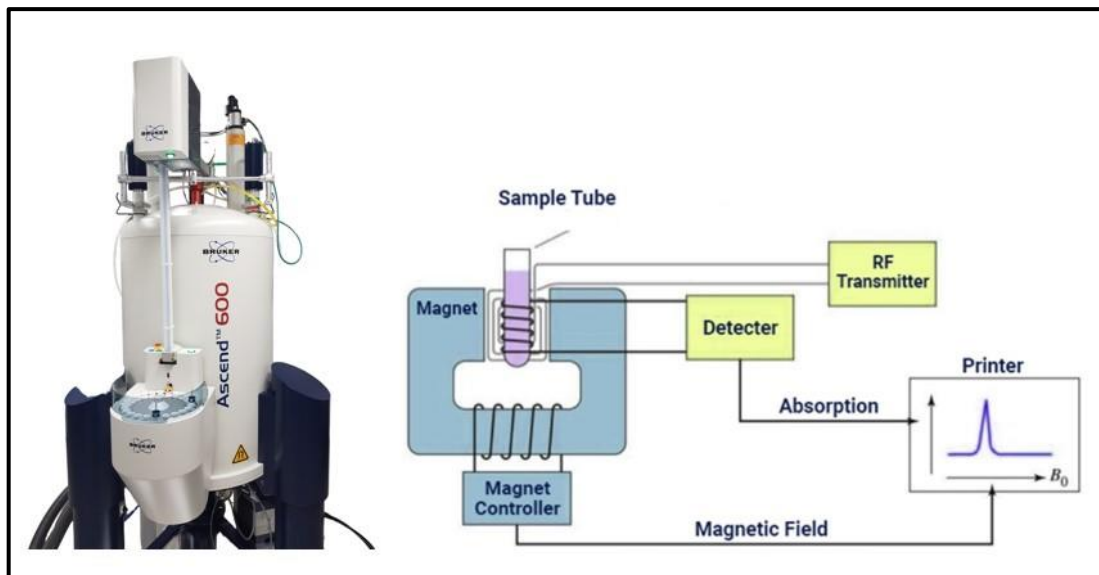


Figure 14: Working Mechanism of NMR

H-NMR is done to confirm the synthesis of copolymer. Different resonance spectra for the copolymers in different environments than the monomers can be seen in the H-NMR spectra of copolymers. The shift of the peak caused by the synthesis of the copolymers can be observed in the NMR spectra which supports the work done further.

3.3.3 Thermogravimetric Analysis (TGA)

A typical TGA analysis is done on a working principle where mass loss has occurred if a thermal event causes the loss of volatile materials. Chemical reactions including combustion causes mass losses, whereas physical changes such as melting are not associated with mass loss. A typical TGA plots the mass loss of sample against temperature or time to show the event of loss of components during a thermal exposure such as loss of plasticizers or solvents, hydration water, and decomposition of the material[40].

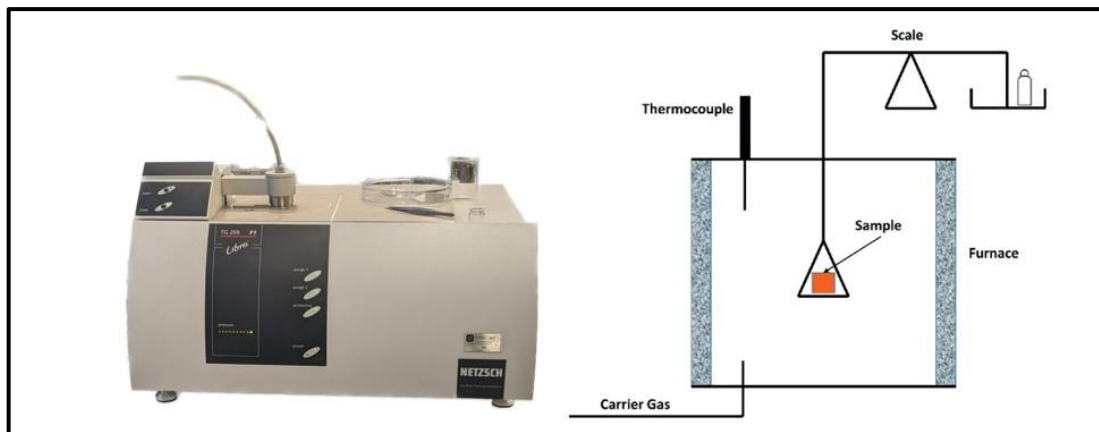


Figure 15: Working Mechanism of TGA

TGA of the zwitterionic copolymers was done to analyze the mass loss of the individual monomers present inside the copolymers with varied molar ratios. In addition, they can also give the quantitative analysis of the copolymer composition when compared with other spectroscopic techniques for composition analysis.

3.3.4 Scanning Electron Microscopy (SEM)

SEM is characterized by generating largely magnified image using electron beam instead of the conventional method. The electron gun which is fitted placed at the top of the microscope is responsible for producing an electron beam which goes vertically through the microscope and is then held within a vacuum. This beam passes through electromagnetic fields and lenses and is focused down towards the sample. As this beam hits the samples, X-ray and electrons are ejected which is collected by the detector. The detector collects all the back-scattered electrons, secondary electrons and the X-rays. These electrons are then converted into a signal that is sent to a screen which allows them to be imaged[41].

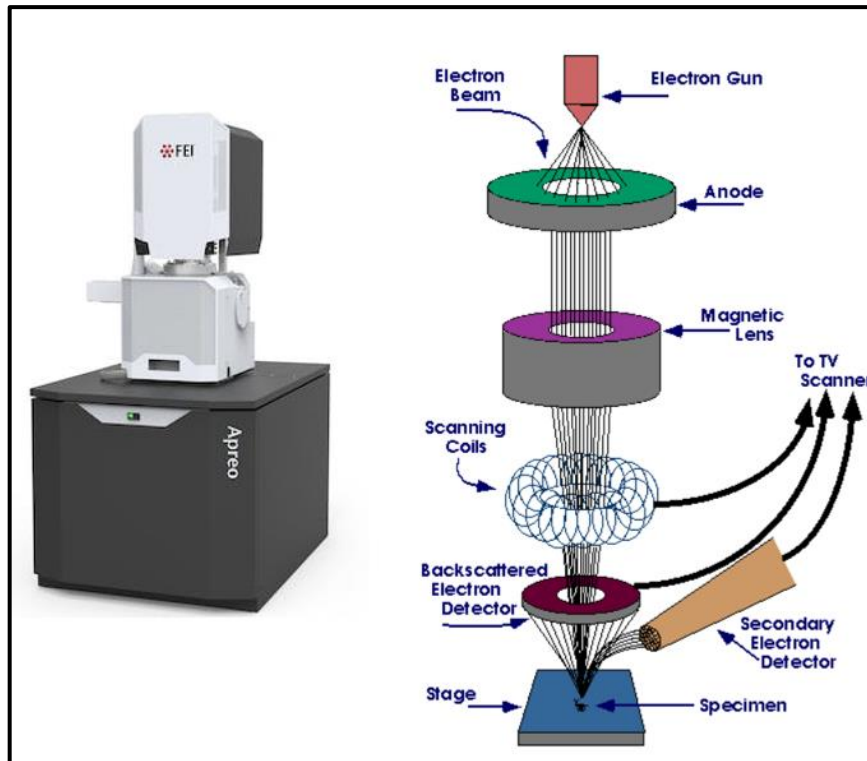


Figure 16: Working Principle of SEM

Surface morphologies of the membranes were analyzed using SEM where the top section of the Nexar membranes as well as the cross sectional view of the thus formed membranes were imaged to observe the assembly formed by the BCP. In the case of the zwitterionic modified PEI membranes, the cross sectional view of the membranes were imaged to observe the changes caused by the surface modification by the copolymer.

3.3.5 Atomic Force Microscopy (AFM)

AFM dimension icon was used to analyze the surface roughness parameters of membranes. The probe performs the scanned sample surface, the contact force which generated between the probe tip and scanned surface causes a small elastic deflection of cantilever. This cantilever deflection is then measured through reflection of a laser beam to a photodetector which records the movement the laser beam reflected. The signal which

is generated from the photodetector is converted to a topographic image of the sample scanned surface[42].

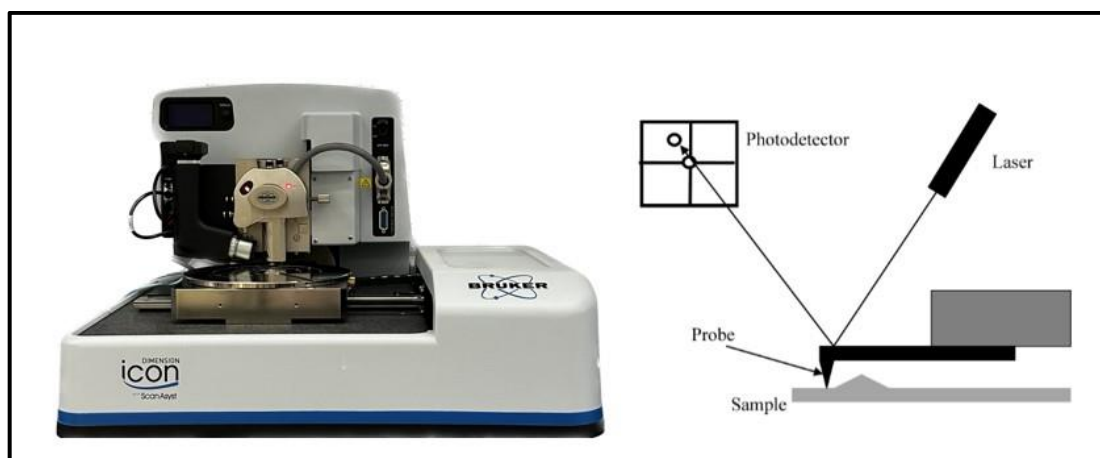


Figure 17: Working Principle of AFM

This AFM dimension icon perform imaging techniques on the sample that are placed inside the chamber and the range of imaging is up to 210mm in diameter. AFM of the membrane modified can be analyzed and the effect of the modification on the surface topography can be studied through various surface roughness parameters.

3.3.6 Drop Shape Analyzer (DSA)

Water contact angle can be described as the angle formed between a liquid droplet and the active top layer surface of a membrane. This can be determined through the drop shape analyzer (DSA). Liquid molecules tends to generate angles as they interact with molecules of solid, liquid, and gas at a three phase boundary[43].

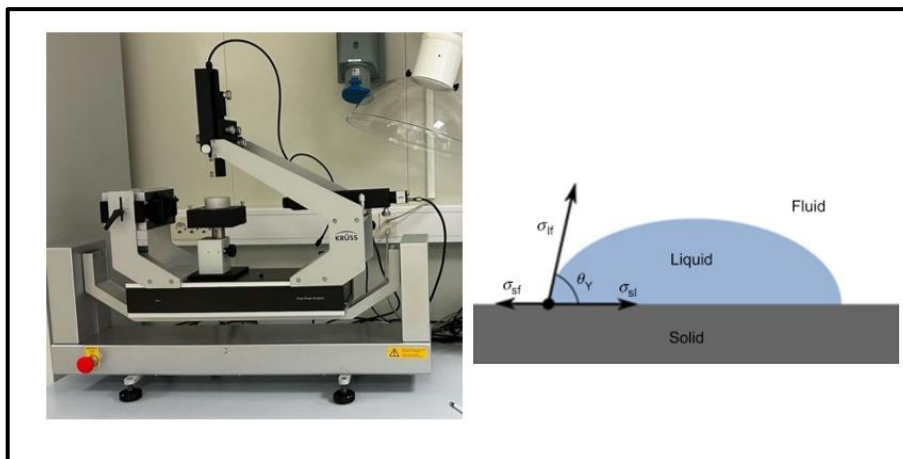


Figure 18: Working mechanism of DSA

The wetting ability of the polymer surface hydrophilicity can be determined by the contact angles. Angle formed between the active top layer and a liquid droplet can give the hydrophilic measure of the materials as an angle less than 90 the is hydrophilic whereas, contact angles greater than 90 degrees are deemed to be on the hydrophobic side.

3.3.7 Water Uptake

The hydrophilicity of the membrane can also be determined using a parameter named water uptake. To calculate the water uptake, three sets of $1 \times 1 \text{ cm}^2$ membrane area was taken. Samples were oven dried for 6 hours at 60°C for the removal of trapped moisture and weighed. The samples were then immersed in DI water for 48 hours and weighed again by wiping the surface water. Then the water uptake was calculated using the following equation[44]

$$\text{Water Uptake}(\%) = \frac{W_{\text{wet}} - W_{\text{dry}}}{W_{\text{dry}}} \times 100$$

3.4 Dead-end Filtration

A unit HP4750- Sterlitech with an operative membrane area of 0.00146 m^2 Dead end stirred batch cells were used in membrane rejection experiments to test the changes cause

by the solvent on morphology of membrane and to test the salt rejections as well as the antifouling properties.

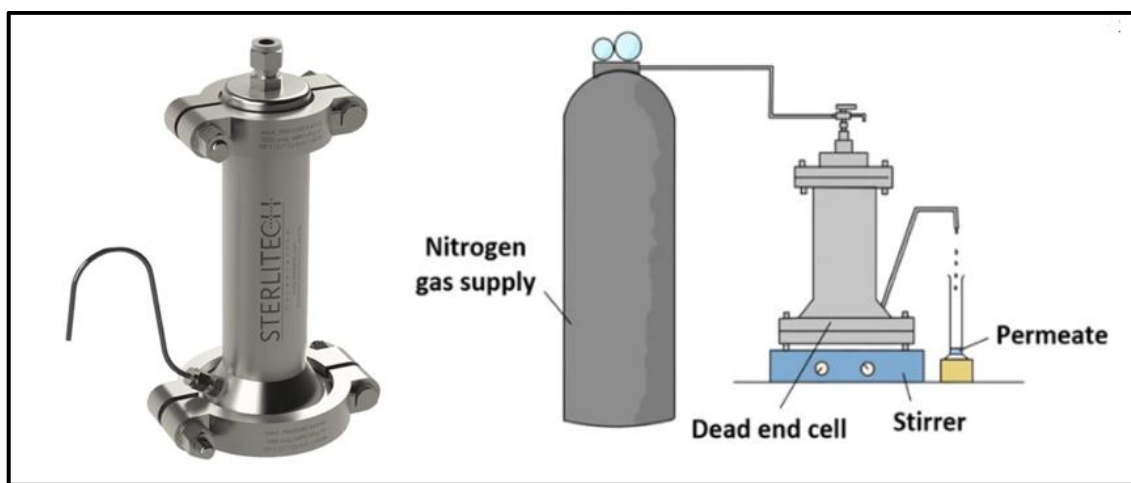


Figure 19: Working of Dead-end Filtration process

The experimental setup comprised of the following components

- a nitrogen cylinder to purge the cell and provide the desired transmembrane pressure
- dead-end vessel
- membrane filtration template of known area
- polymeric membrane
- permeate container

The feed stream for dead-end filtration is DI water and synthetic wastewater. Initially, the system was allowed to run for almost 10 minutes to stabilize its flow and pressure. Operating pressure for the dead-end filtration was 2 bar. Experiment was conducted at room temperature for 1 hour for short term experiments to achieve the constant flux. Finally, permeate was collected in beaker for every 10 minutes.

3.4.1 Pure Water Permeability (PWP)

Pure water permeability measurement was performed using the dead-end filtration equipment (Sterlitech HP 4750, USA). The feed stream for pure water permeability measurement was DI water. Initially, the system was allowed to run for almost 10 minutes

to stabilize its flow and pressure. Operating pressure for the dead-end filtration was 10 bar. Experiments were conducted at room temperature for 1 hour to achieve a constant flux. Finally, permeate was collected in a container for each run.[45].

$$j = \frac{V}{A \times T}$$

Where, J is the flux, L/m² h, T is the time in hours, A is the total area of the membrane in m², and V is the Volume of the permeated water in Liters.

The permeability (Lm⁻²h⁻¹/bar) was calculated using the equation below

$$Permeability = \frac{Flux}{Pressure}$$

3.4.2 Arsenic and Selenium Rejection

The feed stream for arsenic and selenium rejection measurements was prepared using 100ppm of both arsenic and selenium in ratio (1:1). This mixed feed was then subjected to the membranes via dead end filtration. The mode of experimentation was similar to that done for the pure water permeability measurement. The permeates of the samples were then analyzed for salt rejection by determining the concentrations of arsenic and selenium in the permeate through atomic absorption spectroscopy (AAS Vario 6, Analytik Jena AG (3111B APHA)).

The rejections (%) can be then calculated as follows

$$R(\%) = 1 - \left(\frac{C_p}{C_f} \right) \times 100$$

C_p and C_f are the concentrations of the solute in the permeate and feed sides[30]

Chapter 4

Results and discussion

4.1 Polymer characterization

The synthesis of the zwitterionic random copolymer P[MPC-co-AEMA] was done through single-step one-pot free-radical polymerization between MPC and AEMA using AIBN initiator. The conformation of the copolymer synthesis is primarily discussed in terms of the characteristics of both the monomers which they impart to the copolymer. The hydrophilic chain MPC and amino chains of AEMA are discussed and analyzed in the section below using FTIR, NMR and TGA to confirm the presence of the above mentioned properties in the copolymer.

4.1.1 Fourier Transform Infrared Spectroscopy

The FTIR spectra of the copolymer with respect to the monomer in Fig. 20 confirms the chemistry of the copolymer. The strong peak that appears around 1728cm^{-1} is assigned to the C=O of the ester group, whereas the peaks appearing at 1240 , 1089 , and 970cm^{-1} are attributed to POCH₂ and C⁺CH₃ groups, respectively. These peaks suggest the presence of the MPC segments in the copolymer. The absorption at 1621 and 700cm^{-1} corresponds to the NH₂ groups that comes from the AEMA segments[34].

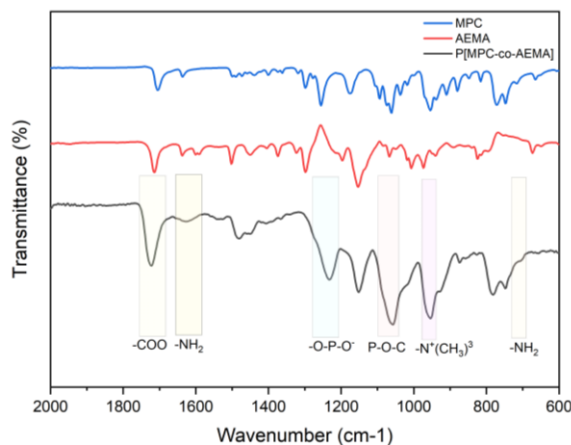


Figure 20: FTIR spectra of the P[MPC-co-AEMA] copolymer and monomers

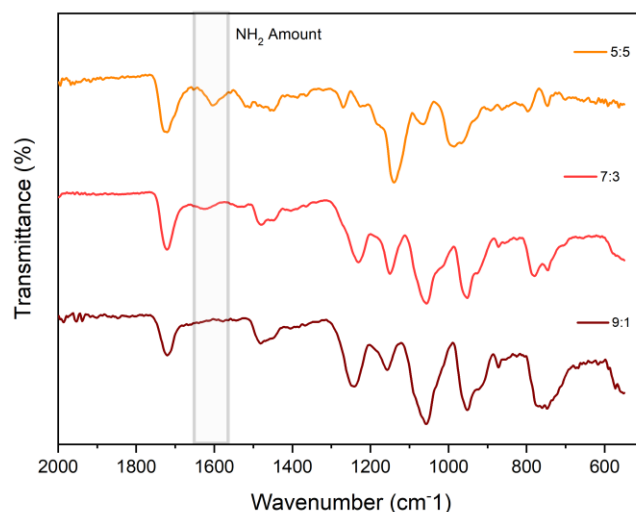


Figure 21: FTIR spectra of the P[MPC-co-AEMA] copolymer with different molar ratios

The presence of these peaks coming from both monomers can also be seen in Figure 21 where the FTIR spectra of the copolymer with different molar ratio is shown. By increasing the MPC content of the copolymer, the hydrophilic properties of the copolymer are intended to be improved and at the same time the amino segment of the copolymer coming from AEMA is also to be kept intact. The intensity of the amino group is decreasing by decreasing the AEMA amounts in the copolymerization reaction[7]. Therefore, an ideal molar ratio based upon the improved hydrophilic and antifouling properties of the membranes will decide the ideal molar ratio of the copolymer.

4.1.2 Nuclear Magnetic Resonance

Proton nuclear magnetic resonance (^1H NMR) spectra of P[MPC-co-AEMA] further provides the copolymer analysis. This compositional analysis of the copolymer was done by H-NMR spectroscopy where D₂O was used as a solvent. The vinyl resonance of the monomers which appears in the range of 5.3-5.8 ppm to the methyl resonance of the polymer that appears between 0.5-1.4 ppm is compared for the copolymer synthesis. [46].

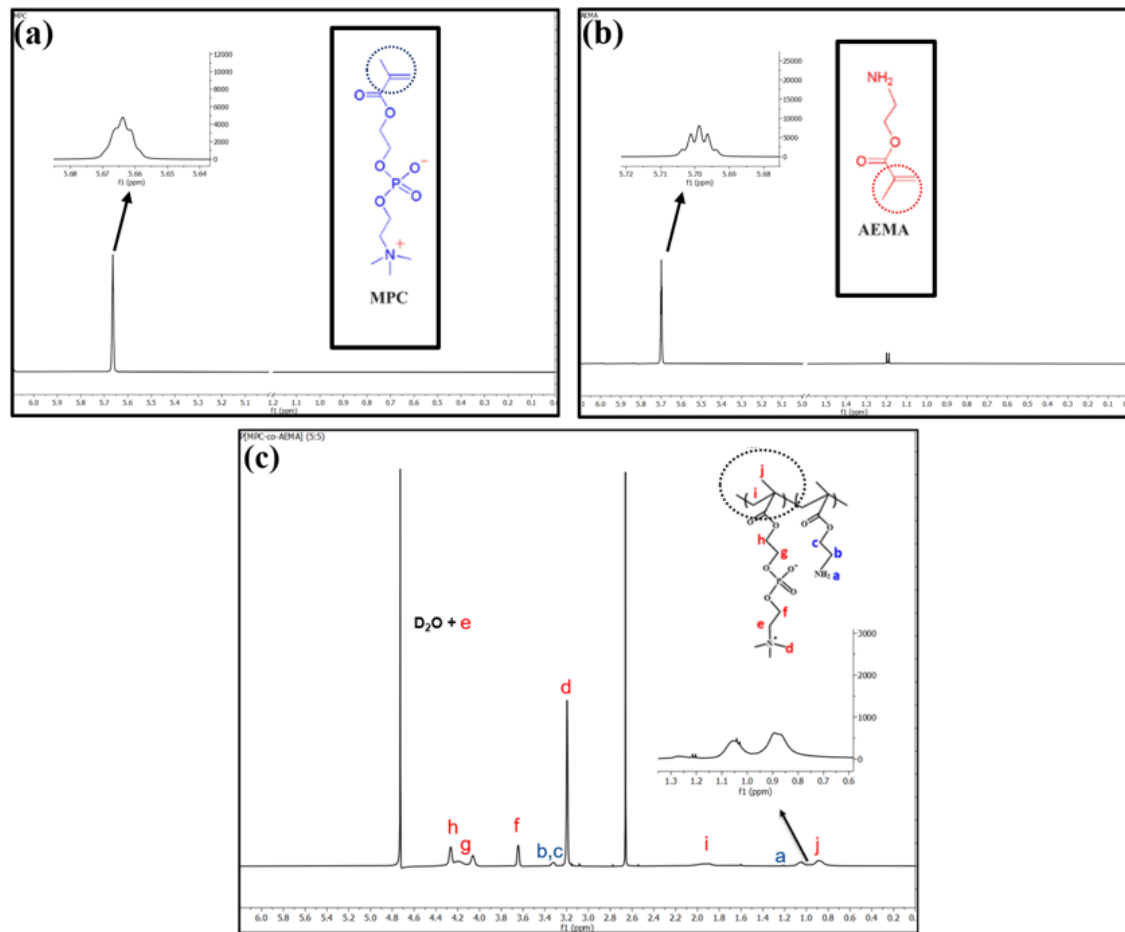


Figure 22: Proton nuclear magnetic resonance (¹H NMR) spectra of (a) MPC (b) AEMA (c) P[MPC-co-AEMA]

The NMR spectra of the copolymer as shown in Fig. 22 further confirms the synthesis of the zwitterionic copolymer. Different peaks corresponding to the different proton environments can be seen as per the chemical structure of the copolymer.

4.1.3 Thermogravimetric Analysis

Thermogravimetric analysis of the copolymers with different molar ratio of both the monomers was performed as shown in Figure. TGA curves also confirms the synthesis of the copolymer where two different degradation curves corresponding to the degradation temperatures of both the monomers are formed. The initial weight loss until 100°C is because of the hygroscopic moisture and complexes bound water released. Increasing the molar ratio of the MPC content is visible in the TGA curves where the curves shift towards

the right in the MPC degradation section which starts from 250°C till 350°C. Afterwards the AEMA segment of the copolymer undergoes degradation.

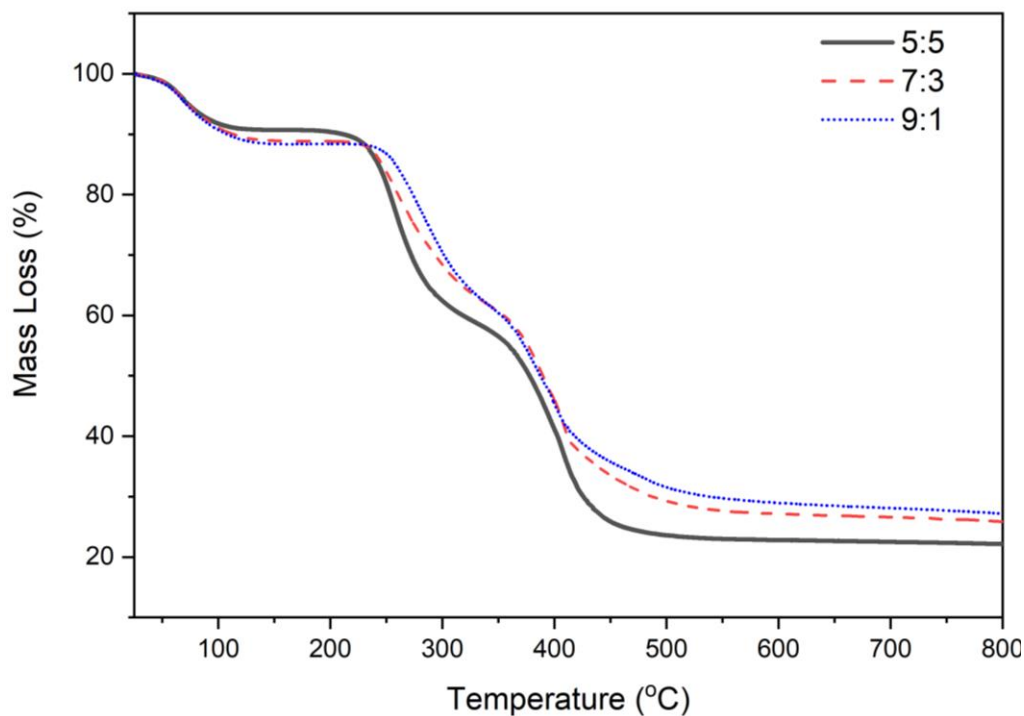


Figure 23: TGA curves of the P[MPC-co-AEMA] copolymer with different molar ratios

4.2 Membrane Characterization

4.2.1 Fourier Transform Infrared Spectroscopy

ATR-FTIR characterization was performed to investigate the chemical structures of the prepared Nexar nanofiltration membranes. The spectrum shows a strong peak in the range of 1026.59-1241.80 cm^{-1} in both membranes resulting from the symmetrical and asymmetrical stretching of SO_3^- . This band confirms the Nexar presence in the membranes. C-S styrene band can be observed in the range of 586.12-836.45 cm^{-1} [47]. The medium peak of C-H bending for aromatic compound is observed at 1635.62 and 1656.30 cm^{-1} in THF and IPA/Tol blend membrane respectively. Peaks appearing at 2921.78 and 2920.26 cm^{-1} correspond to the C-H bond in THF and IPA/Tol blend membrane respectively[48]. The presence of peak around the range of 900 cm^{-1} is due to the presence

of the POSS nanoparticles in the Nexar membranes responsible for imparting the hydrophilic properties to the nanocomposite membranes.

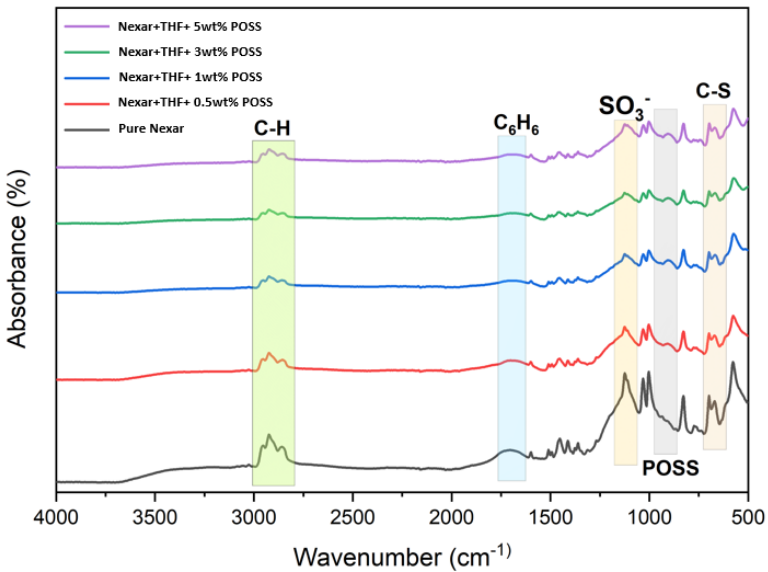


Figure 24: FTIR Spectra of Nexar membranes with THF as solvent

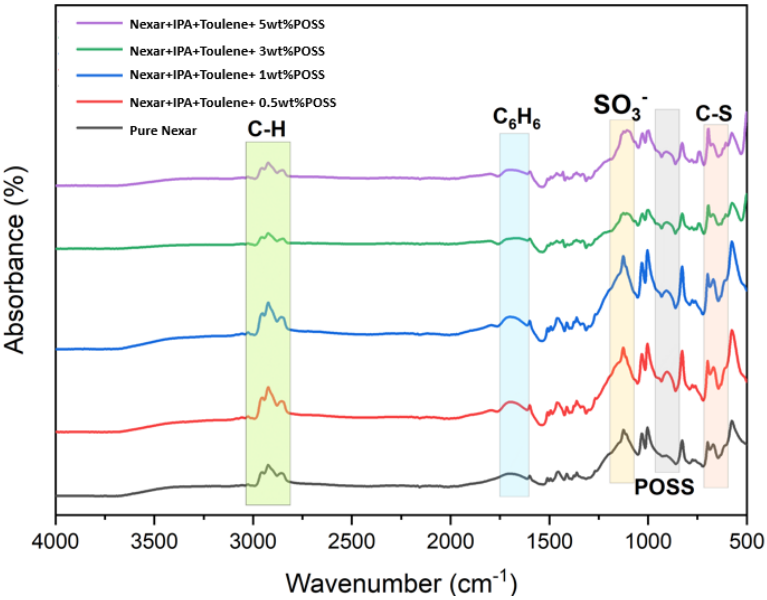


Figure 25: FTIR Spectra of Nexar membranes with IPA and Toluene as solvent

ATR-FTIR characterization was done to determine the of the prepared chemistry of the PEI and modified membranes. As shown in the Figure 26 the FTIR spectra of the membranes when modified with the random zwitterionic copolymer the peaks from the copolymer comprising of both MPC and AEMA segment appears confirming that the amino groups responsible for the linkage are also present along with the hydrophilic MPC functional groups. The peaks at 1240, 1090, and 970 cm^{-1} were attributed to the O-P=O^- and $\text{N}^+(\text{CH}_3)$ groups, indicating the presence of MPC segments on the reacted membrane surface. The peaks assigned to 1621 cm^{-1} and 700 cm^{-1} is attributed to that of AEMA segment linked to the PEI membranes[7].

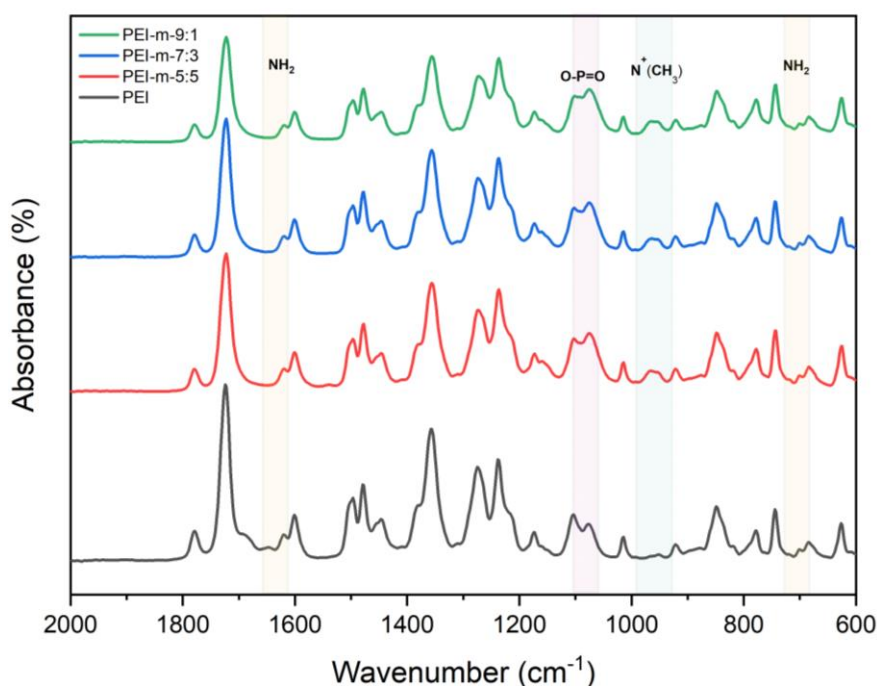


Figure 26: FTIR spectra PEI-m-P[MPC-co-AEMA] membranes with water and TEA

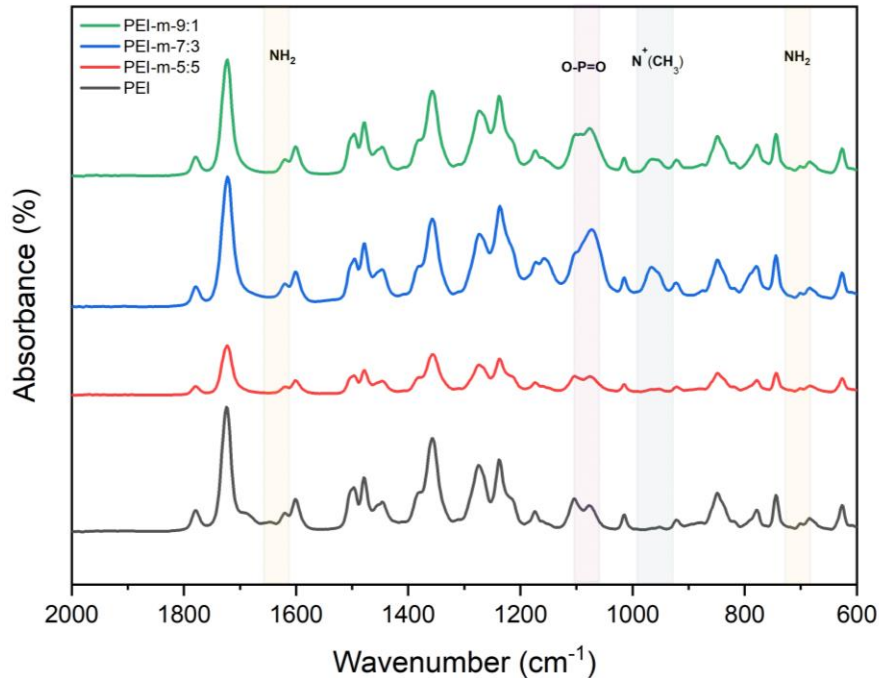


Figure 27: FTIR spectra PEI-m-P[MPC-co-AEMA] membranes with water and IPA

4.2.2 Scanning Electron Microscopy

Surface morphologies of the membrane is shown in Fig.28. Top and cross sectional imaging of the membranes are done along with the EDX analysis. In Fig.28(i)a the top active layer of Nexar membrane having IPA+Toluene as solvents is shown. The membrane exhibits a smooth surface without pores [49]. The cross-sectional imaging of the same membrane shown in Fig28(i)b illustrates the internal dense structure of the membrane and shows a width of $18.12 \pm 0.93 \mu\text{m}$. The width of the Nexar membrane with 0.5wt% POSS loading increases giving its value of $31.08 \pm 0.43 \mu\text{m}$ as shown in Fig.28(ii)b. The variation in the width can be attributed to the nanofiller loading. Since, with POSS incorporation the cross-sectional width of the membrane increases. Higher POSS loading can lead to agglomeration or non-uniform dispersion of the POSS nanoparticles[6]. This will cause increased cross-sectional thickness which can result in the loss of flux. EDX analysis of the pure Nexar membranes and POSS incorporated membranes is done as shown in Fig.28(i)c and Fig. 28(ii) c respectively. The presence of

silicon in the POSS incorporated membranes can be seen in the EDX spectra shown in Fig. 2(ii) c. This can further confirm the presence of the nanofiller in the membrane.

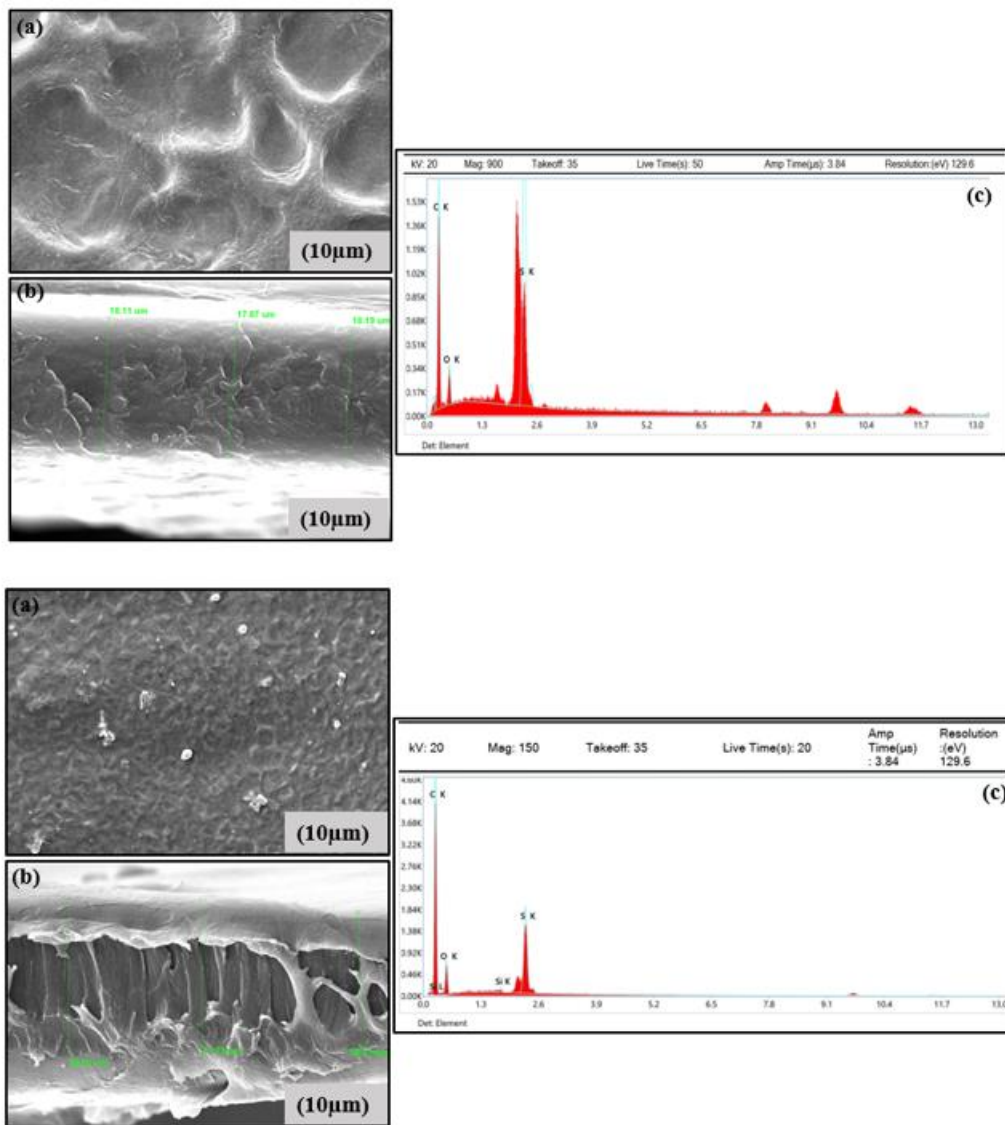


Figure 28: SEM images of (i) Nexar membranes with IPA and Toluene as solvent (a) Top Section (b) Cross-section (c) EDX analysis (ii) 0.5wt% POSS incorporated Nexar membranes with IPA and Toluene as solvents (a) Top Section (b) Cross-section (c) EDX analysis

The cross-sectional structures of all the prepared membranes were investigated using SEM. The influence of the modification of the membranes with P[MPC-co-AEMA] on the resultant membrane structure.

As shown in Figure 28, the cross-sectional view of the PEI membranes and the copolymeric modified membranes are shown. The formation of the hydrophilic layer can be visualized from the cross-sectional view resulting in the change in the morphology of the membrane. The formation of these channels further facilitates the flux through the membrane which can be seen in the membrane flux when subjected to pure wastewater.

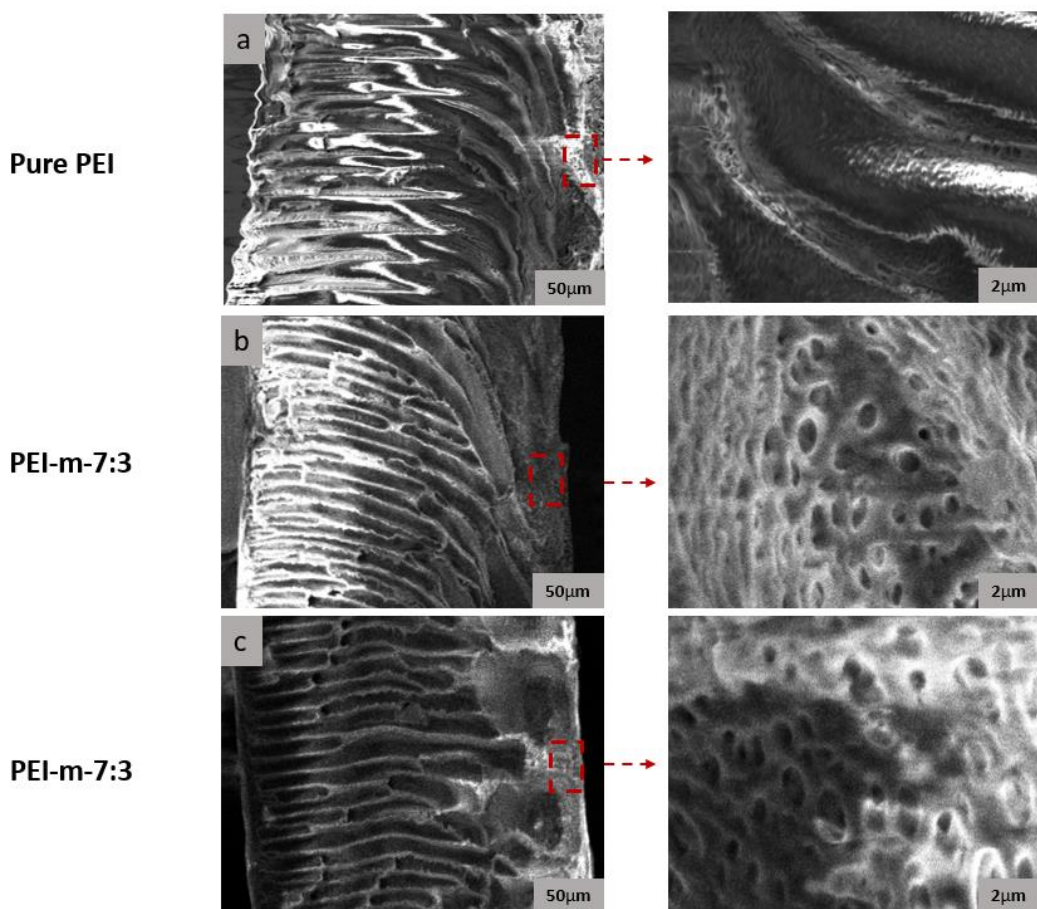


Figure 29: Cross sectional SEM images of (a) Pure PEI (b) PEI-m-P[MPC-co-AEMA] (7:3) with water and TEA (c) PEI-m-P[MPC-co-AEMA](7:3) with water and IPA

4.2.3 Atomic Force Microscopy

Surface roughness parameters of the Nexar membranes were determined by AFM. The scan size of the membranes was 1 by 1 μm , 3D AFM photos of the top surfaces of all the membranes were acquired. On the surface topography, the light parts defined the heights while the dark regions revealed depths. As seen in Table 2 and 3 the surface roughness parameters were measured. Roughness average (R_a), Root mean squared roughness (R_{rms})

and Maximum roughness (R_{max}) were also measured for these membranes. With increase of the POSS loadings the surface roughness parameters were seen to be increasing. This can further be extended to the agglomeration of the POSS nanoparticles with higher loadings since they tend to accumulate when loaded in larger amounts.

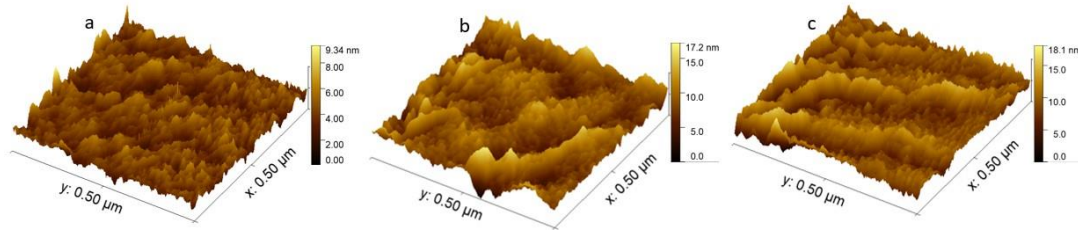


Figure 30: AFM images of (a) Pure Nexar (b) 0.5wt% POSS (c) 5wt% POSS with THF as solvent

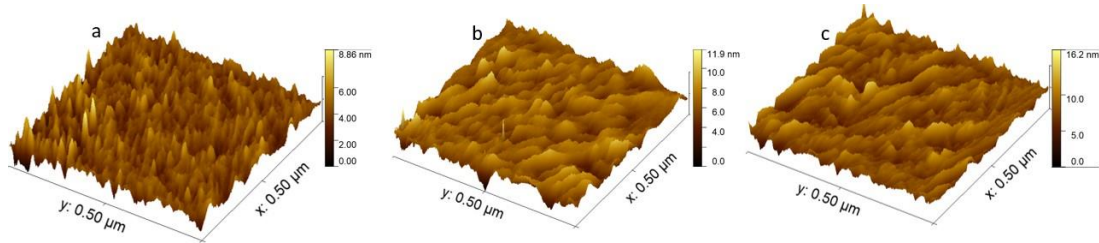


Figure 31: AFM images of (a) Pure Nexar (b) 0.5wt% POSS (c) 5wt% POSS with IPA and Toluene as solvent

Table 2: Surface roughness parameters determined by AFM for Nexar membranes with THF as solvent

Membranes	Nexar	0.5wt%	5wt%
Roughness average (R_a) (nm)	0.238	0.409	0.650
	± 0.0433	± 0.0343	± 0.0754
Root mean squared roughness (R_{rms}) (nm)	0.358	0.526	0.776
	± 0.0212	± 0.0044	± 0.0322
Maximum roughness (R_{max}) (nm)	2.163	3.321	4.125
	± 0.0456	± 0.0323	± 0.0524

Table 3: Surface roughness parameters determined by AFM for Nexar membranes with THF and IPA+Toluene as solvents

Membranes	Nexar	0.5wt%	5wt%
Roughness average (R_a) (nm)	0.3873 ±	0.472 ±	0.7995 ±
	0.0432	0.055	0.1043
Root mean squared roughness (R_{rms}) (nm)	0.665 ±	0.724 ±	1.060 ±
	0.456	0.0993	0.1224
Maximum roughness (R_{max}) (nm)	4.601 ±	6.1679 ±	8.198 ±
	0.0556	0.2544	0.9345

Similar, for the surface topography of the PEI membranes modified with the copolymer, the surface roughness parameters were measured. Roughness average (R_a), Root mean squared roughness (R_{rms}) and Maximum roughness (R_{max}) were also measured for these membranes. From Table 4 and 5 it can be seen, with increasing the molar ratio the roughness average as well as the maximum roughness is increasing. This can be attributed to the grafting copolymer concentration which is varied and employed surface chemical modification process[5]. In comparison to the surface roughness of the pure PEI, surface roughness for the copolymer modified membranes increases, which can be deemed better in terms of filtration processes[50].

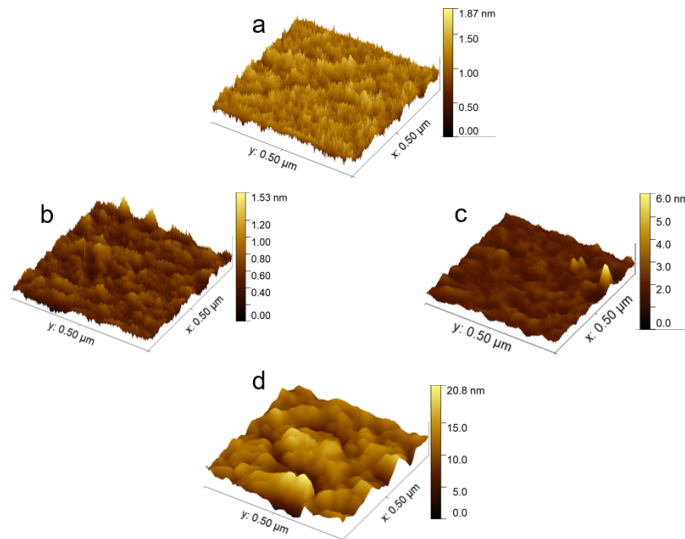


Figure 32: AFM images of (a) Pure PEI (b) PEI-m-P[MPC-co-AEMA] (5:5) with water and TEA (c) PEI-m-P[MPC-co-AEMA] (7:3) with water and TEA (d) PEI-m-P[MPC-co-AEMA] (9:1) with water and TEA

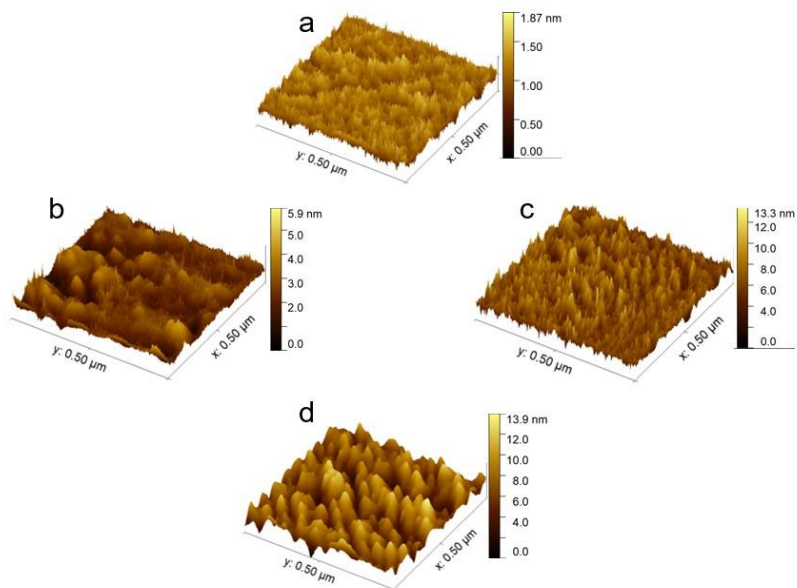


Figure 33: AFM Images of (a) Pure PEI (b) PEI-m-P[MPC-co-AEMA] (5:5) with water and IPA (c) PEI-m-P[MPC-co-AEMA] (7:3) with water and IPA (d) PEI-m-P[MPC-co-AEMA] (9:1) with water and IPA

Table 4: Surface roughness parameters determined by AFM for PEI-m-P[MPC-co-AEMA] with Water and IPA

Membranes	PEI	5:5	7:3	9:1
Roughness average (R_a) (nm)	0.0513 ± 0.0034	0.0513 ± 0.0034	0.0591 ± 0.0134	0.1214 ± 0.0636
	0.0627 ± 0.0035	0.0627 ± 0.0035	0.0725 ± 0.0163	0.1704 ± 0.1116
Root mean squared roughness (R_{rms}) (nm)	0.3141 ± 0.0118	0.3141 ± 0.0118	0.3544 ± 0.0523	1.0271 ± 0.1213

Table 5: Surface roughness parameters determined by AFM for PEI-m-P[MPC-co-AEMA] with Water and TEA

Membranes	PEI	5:5	7:3	9:1
Roughness average (R_a) (nm)	0.0513 ± 0.0034	0.1771 ± 0.0511	0.5017 ± 0.14429	0.6069 ± 0.1754
	0.0627 ± 0.0035	0.2248 ± 0.0644	0.6621 ± 0.1836	0.7717 ± 0.2195
Root mean squared roughness (R_{rms}) (nm)	0.3141 ± 0.0118	1.1679 ± 0.2299	3.9195 ± 0.9779	4.0957 ± 1.4417

4.2.4 Water Contact Angle

The hydrophilic properties of the Nexar membranes were determined by measuring their WCA for 2 min continuously. Pure Nexar membranes with both THF and IPA/Toluene membrane gave a higher WCA in borderline hydrophilic range around 85° and the reduction of WCA over 2 min was very small. The initial lowest WCA is for 0.5wt%POSS in both THF and IPA/Toluene solvents. It starts around 77° and decreases to 72° for nearly both. For higher POSS loadings the decrease in the water contact angles over the period of 2 min can be seen with higher initial contact angles when compared to the 0.5wt POSS. This may be hypothesized that higher loading causes an agglomeration of POSS. This agglomeration may cause sudden trends.

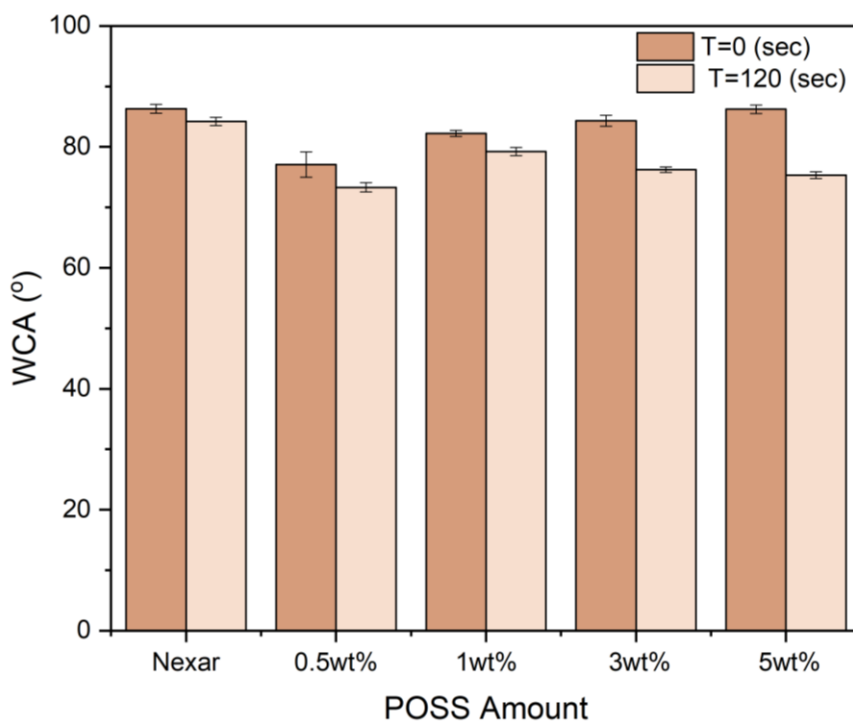


Figure 34: Water Contact Angles of Nexar membranes with THF as solvent

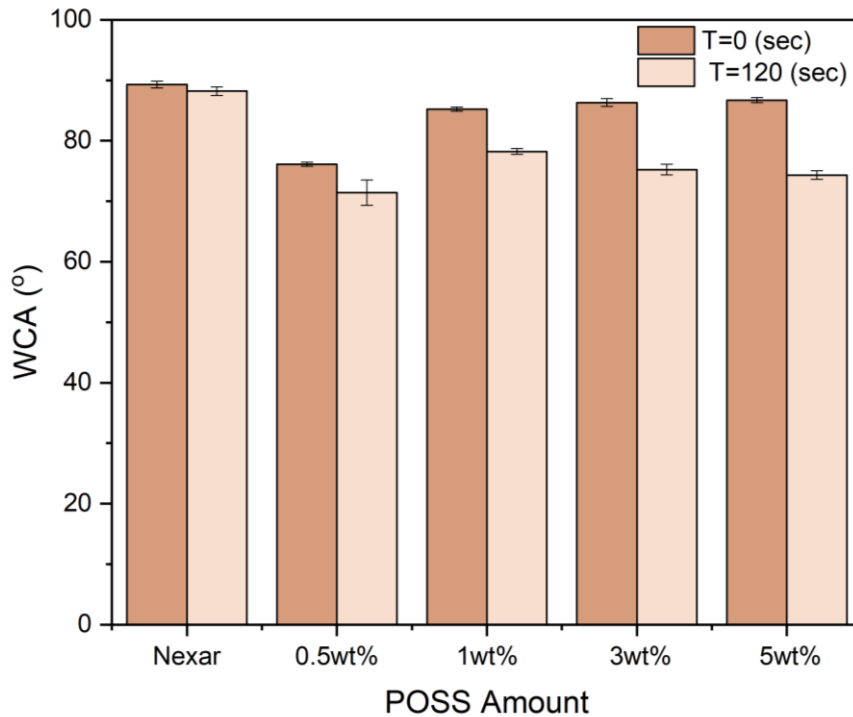


Figure 35: Water Contact Angles of Nexar membranes with IPA+Toluene as solvent

The hydrophilic properties of the PEI and copolymer modified membranes were determined by measuring their WCA for 2 mins. Pure PEI membrane gave a WCA of approximately 70° and the reduction of WCA over 2 min was very small. After the membrane was modified with P(MPCAEMA), the surface hydrophilicity of the membranes noticeably increased[7]. As shown in Figure 35 and 36, the initial WCAs of PEI-m-P[MPC-co-AEMA] decreased from 70° with different copolymer ratio. The WCA for 5:5, 7:3 and 9:1 gradually decreased from the initial values over 2 min time. The WCA of the membrane modified with 7:3 copolymer had the lowest initial WCA for both systems i.e., 29° for water and TEA and reduced to 21° after 2 mins. Similarly for water and IPA, the initial WCA was 26° and decreased to 22° . This decrease in the contact angle can be explained in terms of MPC being more dominant in 7:3 copolymer with AEMA in sufficient amounts to provide the linkage to the membrane surface. In 9:1 copolymer, insufficiency of AEMA may well be the reason of the lesser hydrophilicity as compared to the membranes modified with 7:3 copolymer.

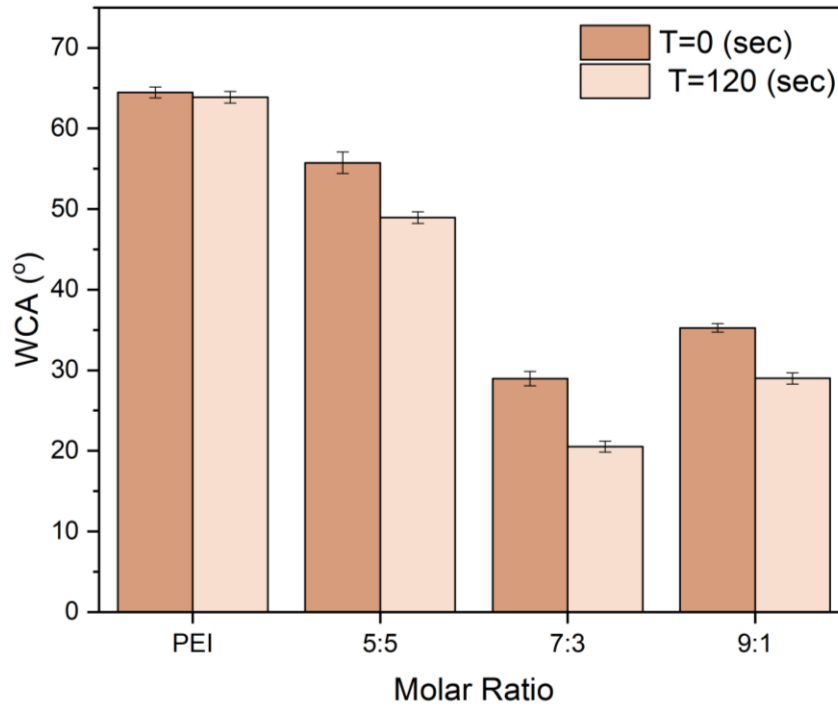


Figure 36: Water Contact Angles of PEI-m-P[MPC-co-AEMA] membranes with Water+TEA

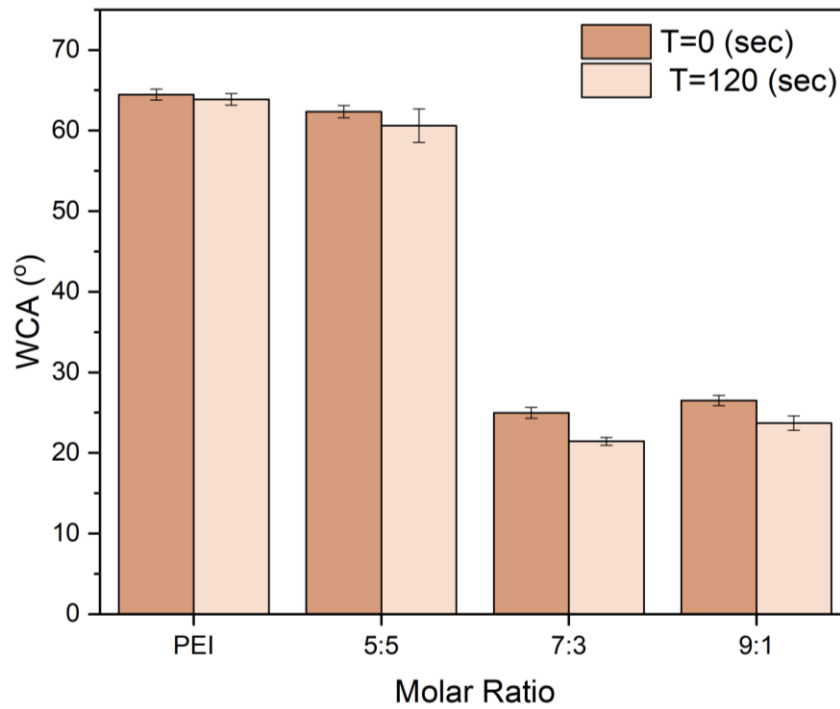


Figure 37: Water Contact Angles of PEI-m-P[MPC-co-AEMA] membranes with Water+IPA

4.2.5 Water Uptake

Water uptake of the Nexar membranes were also in correspondence with the other results. The maximum water uptake was 170% for the 0.5wt% POSS loading. The water uptake for IPA/toluene solvents prepared membranes were found to be more than those for the THF solvent[44].

For the PEI membranes, the water uptake was in a similar trend with PEI membranes modified with 7:3 copolymer exhibiting a higher uptake as compared to the control and membranes with other copolymer modification. The water uptake for both modification systems are marginal for 7:3 membrane modification. PEI-m-P[MPC-co-AEMA] with water and TEA gives water uptake up to 238% whereas water and IPA gives 222%.

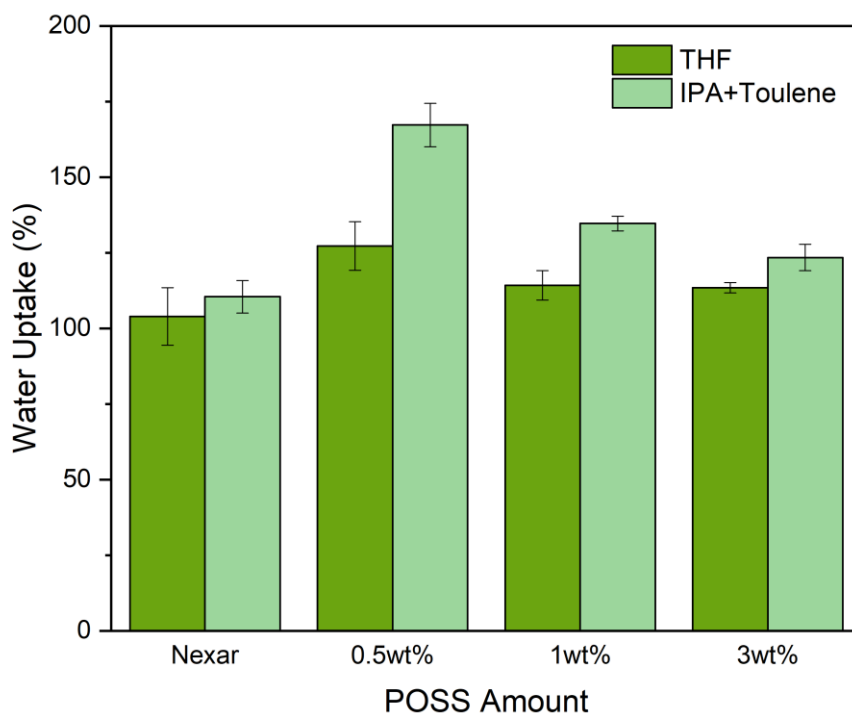


Figure 38: Water Uptake for Nexar membranes with THF and IPA+Toluene as solvents

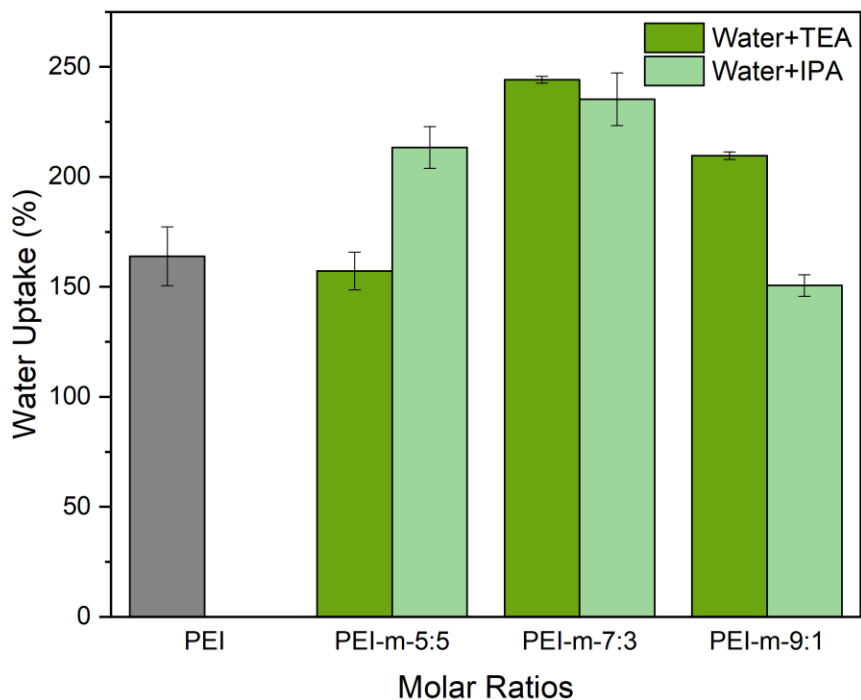


Figure 39: Water Uptake for PEI-m-P[MPC-co-AEMA] with Water+TEA and Water+IPA

4.3 Membrane Testing

4.3.1 Pure Water Permeability

Pure Water Permeability of the Nexar membranes were calculated as shown in Fig.40. The membrane with 0.5wt% POSS loading in IPA+Toluene showed the highest PWP of 95 LMH/bar. Increasing in the POSS loading decreased the PWP to 33LMH/bar. PWP of the membranes in IPA +Toluene are significantly higher than their respective counterparts in THF. This can be attributed to the self-ordering globular structure synthesized while using IPA+Toluene. In case of THF, the hypothesis of nano-highways seems to constrict the sulfonated middle core reducing the water-selective passage[33]. With further increase in the POSS loading the flux reduced which can be attributed to an increased chain rigidity and decreased chain spacing. This reduced flux can also be due to the addition of POSS nanoparticles over the threshold that may result in an increased mass transport resistance. The non-uniform dispersion of high loading POSS nanoparticles causing agglomeration and reduce the water uptake which correlates to the water uptake in the section above[6].

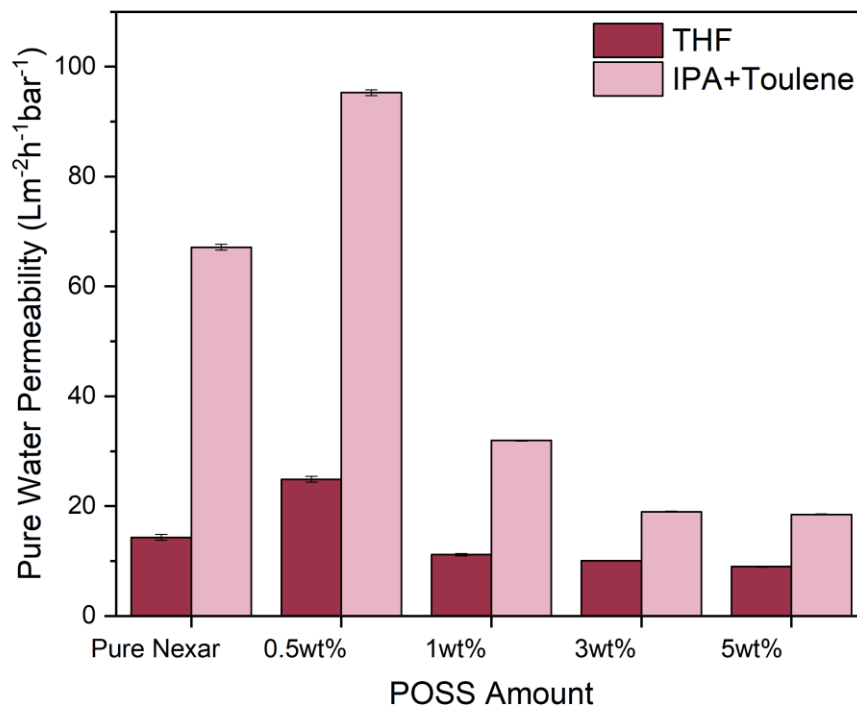


Figure 40: Pure Water Permeability for Nexar membranes with THF and IPA+Toluene as solvents

Similarly, PWP for the PEI modified membranes were also calculated which showed the trend in correspondence to the above mentioned results. The PWP were reported to be high for water and IPA system compared to the water + TEA. The PWP of the membranes modified with 7:3 copolymer with water and IPA gave the highest PWP of $17 \text{ Lm}^{-2}\text{h}^{-1}\text{bar}^{-1}$. With higher molar ratios the PWP declined. The PWP of the membranes with Water and TEA gave considerably low fluxes can be explained in terms of the pore sizes that are reduced when modified using TEA as a catalyst[7].

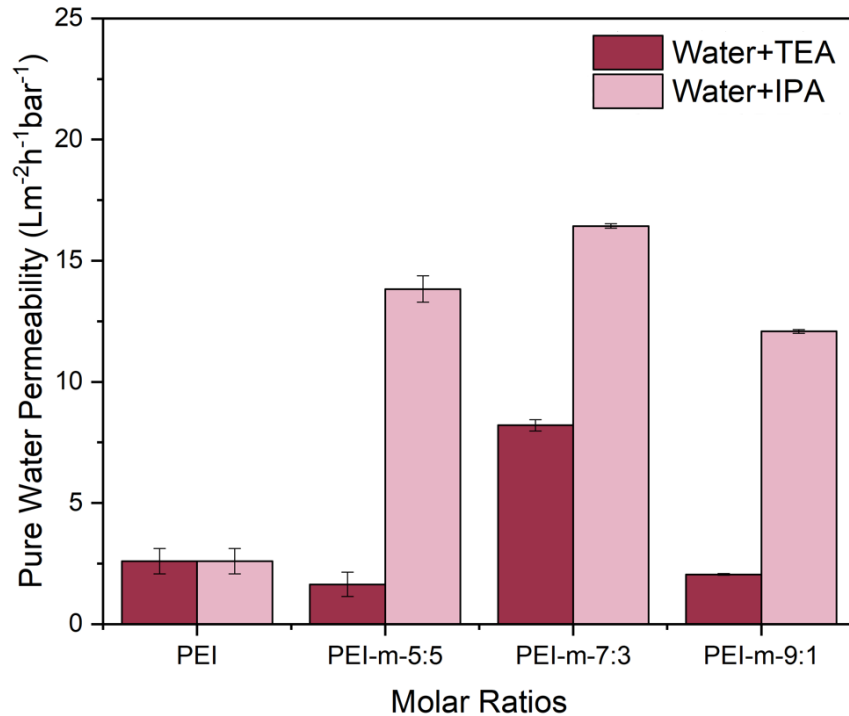


Figure 41: Pure Water Permeability for PEI-m-P[MPC-co-AEMA] with Water+TEA and Water+IPA

Arsenic and selenium rejections for the Nexar membranes were calculated as shown in Fig. 42 (a) and (b). The permeate samples from the dead-end filtration were analyzed for arsenic and selenium concentrations. The rejections for all the membranes seemed to be promising once compared to the literature. For 0.5wt % loadings, the rejections for arsenic were the highest of 98.22% whereas for selenium the rejection was highest with values of 98.05% for IPA and Toluene as solvents. The high values of rejections for 0.5 wt% membranes along with maximum flux as reported in the above section makes it the best performing membrane. With uniform POSS dispersion it serves to act as a nanofiller that also tightens the pores. Thus, aiding to the improved rejections compared to the pure Nexar

membranes[6]

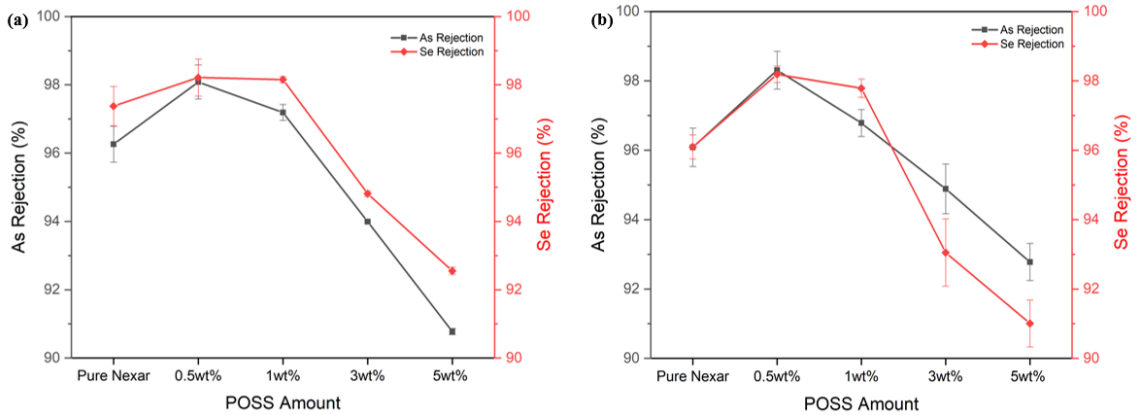


Figure 42: Arsenic and Selenium rejections for Nexar membranes with (a) THF (b) IPA+Toluene as solvents

Rejections for the PEI modified with the copolymer membranes shown in Fig. 43 (a) and (b) were found to be somewhat higher than the above mentioned. For the membranes modified with water+ TEA as a catalyst, the rejection percentages were found out to be higher than those which were modified with IPA and water. The highest rejection for arsenic and selenium were both found out to be with 7:3 copolymer modified membranes giving rejections 99.49% and 98.78% respectively. These enhanced rejections using TEA can be explained in terms of reduced pore size by using TEA instead of IPA with water[7].

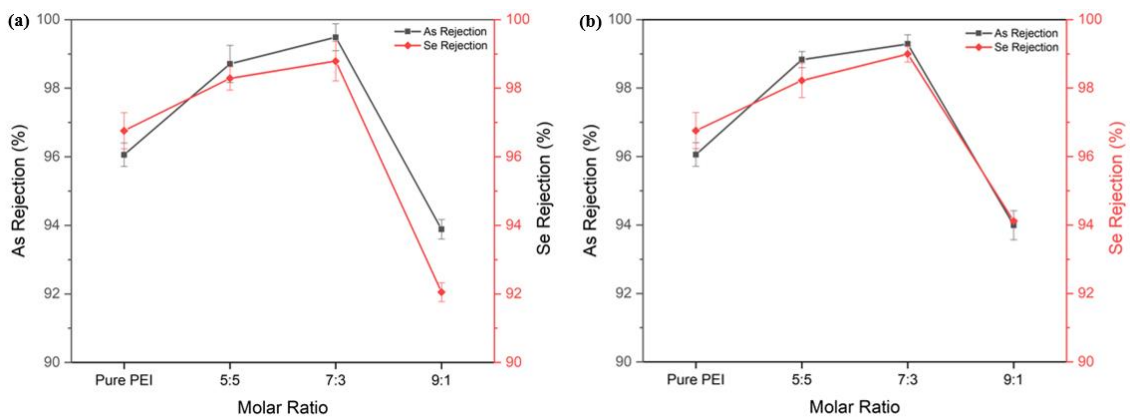


Figure 43: Arsenic and Selenium rejections for PEI-m-P[MPC-co-AEMA] with (a) Water+TEA (b) Water+IPA

Conclusion

In this study we have synthesized and characterized nanofiltration membranes for heavy metals treatment from synthetic wastewater. In the first phase of the research work, a sulfonated block copolymer Nexar was chosen as the polymer and membranes were synthesized using two solvents THF and IPA/Toluene. POSS as an antifouling nanofiller was used to impart its properties to the membrane system. Different loadings of POSS nanoparticles were incorporated into the polymer solution to analyze the effects of the hydrophilic agent in the polymer matrix. After the synthesis of the nanofiltration block copolymeric membranes these were characterized using analytical techniques such as FTIR, AFM, FTIR and WCA which allowed them to be analyzed from macroscopic to microscopic levels. These membranes were then subjected to dead-end filtration to get tested for Arsenic and selenium removal efficiency.

In the second phase of the research work, synthesis of a zwitterionic copolymer was done initially. The synthesis of these new-generation hydrophilic materials was done through one-pot free radical copolymerization. This copolymer consisting of a hydrophilic part MPC and amino linkage AEMA was the focus of study with their molar ratios varied. In this regard, three different molar ratios of MPC:AEMA were synthesized during the copolymer synthesis namely 5:5, 7:3 and 9:1. These copolymers were then characterized to confirm their chemistry as well as determine their composition. This was done using FTIR, TGA and NMR. Next these copolymers were used to modify the surface of PEI nanofiltration membranes. These membranes were allowed to interact with the copolymers in Water and IPA as first medium. Water and TEA as catalysts were also used to allow the surface modification of the PEI membranes. These membranes were also then analyzed using the same above mentioned analytical tools and finally subjected to dead-end filtration to test them for arsenic and selenium rejections.

The last part of the study was the comparative analysis of both works done based on results obtained from both works. In this regard, the first comparison was done by analyzing the contact angles of the membranes. With zwitterionic materials expected to impart its hydrophilic properties to the membranes, the WCA as low as 22° were observed whereas

for the Nexar membranes with POSS incorporated the WCA were not as low. Based on the rejections, the membranes were also compared with the copolymeric membranes modified with water and TEA showing superior results than its counterpart as well as those with POSS incorporated Nexar membranes with rejection of 99.49% and 98.78% for arsenic and selenium respectively. But these enhanced rejections can compromise the high flux rate as seen in the results where the flux of membranes with water and IPA were comparatively higher. Therefore, the need for the optimization of flux and selectivity will be always considered moving forward into such cases

Future Recommendations

- Nexar nanofiltration membranes provides a balance between selectivity and flux. Such properties make it viable for other water treatment application.
- POSS nanoparticles usage can also be extended to other polymer matrices.
- Different functionalized POSS nanoparticles can also be used with Nexar as a hydrophilic nanofiller.
- Zwitterionic copolymers are the next generation of hydrophilic materials. Many of such nature are currently studied and synthesized.
- The interaction of such copolymers with different polymers can be studied since there are number of ways to add such copolymers into polymer matrix.

References:

- [1] Y. He, Y. P. Tang, D. Ma, and T.-S. Chung, "UiO-66 incorporated thin-film nanocomposite membranes for efficient selenium and arsenic removal," *Journal of Membrane Science*, vol. 541, pp. 262-270, 2017/11/01/ (2017).
- [2] S. O. Adio, M. H. Omar, M. Asif, and T. A. Saleh, "Arsenic and selenium removal from water using biosynthesized nanoscale zero-valent iron: A factorial design analysis," *Process Safety and Environmental Protection*, vol. 107, pp. 518-527, 2017/04/01/ (2017).
- [3] V. R. Moreira, Y. A. R. Lebron, L. V. S. Santos, E. Coutinho de Paula, and M. C. S. Amaral, "Arsenic contamination, effects and remediation techniques: A special look onto membrane separation processes," *Process Safety and Environmental Protection*, vol. 148, pp. 604-623, 2021/04/01/ (2021).
- [4] "Polymer Science and Engineering: The Shifting Research Frontiers (1994) National Academies of Sciences, Engineering, and Medicine. 1994. Polymer Science and Engineering: The Shifting Research Frontiers. Washington, DC: The National Academies Press. <https://doi.org/10.17226/2307>," (1994).
- [5] X. Zhang *et al.*, "In Situ Chemical Modification with Zwitterionic Copolymers of Nanofiltration Membranes: Cure for the Trade-Off between Filtration and Antifouling Performance," *ACS Applied Materials & Interfaces*, vol. 14, no. 25, pp. 28842-28853, 2022/06/29 (2022).
- [6] Y. He, Y. P. Tang, and T. S. Chung, "Concurrent Removal of Selenium and Arsenic from Water Using Polyhedral Oligomeric Silsesquioxane (POSS)–Polyamide Thin-Film Nanocomposite Nanofiltration Membranes," *Industrial & Engineering Chemistry Research*, vol. 55, no. 50, pp. 12929-12938, 2016/12/21 (2016).
- [7] P. Zhang *et al.*, "A novel method to immobilize zwitterionic copolymers onto PVDF hollow fiber membrane surface to obtain antifouling membranes," *Journal of Membrane Science*, vol. 656, p. 120592, 2022/08/15/ (2022).
- [8] T. E. o. E. Britannica, " polymerization," (2020).

- [9] S. Majee, G. Halder, and T. Mandal, "Formulating nitrogen-phosphorous-potassium enriched organic manure from solid waste: A novel approach of waste valorization," *Process Safety and Environmental Protection*, vol. 132, pp. 160-168, 2019/12/01/ (2019).
- [10] H. R. Kricheldorf, *Handbook of polymer synthesis*. CRC press, (1991).
- [11] J. K. Stille, "Step-growth polymerization," *Journal of Chemical Education*, vol. 58, no. 11, p. 862, 1981/11/01 (1981).
- [12] P. C. P. Michael M. Coleman, *Fundamentals of Polymer Science: An Introductory Text*, 2nd ed. Routledge, (1998).
- [13] O. Webster, W. Hertler, D. Sogah, W. Farnham, and T. V. RajanBabu, "Group-transfer polymerization. 1. A new concept for addition polymerization with organosilicon initiators," *Journal of the American Chemical Society*, vol. 105, no. 17, pp. 5706-5708, (1983).
- [14] T. P. D. Krzysztof Matyjaszewski, *Handbook of Radical Polymerization*. John Wiley & Sons, Inc., (2002).
- [15] E. S. 1.-G. Marc A. Dube', and Iva'n Zapata-Gonza'lez, " Handbook Of Polymer Synthesis, Characterization, And Processing," A JOHN WILEY & SONS, INC., (2013), ch. Copolymerization.
- [16] R. W. Baker, *Membrane Technology and Applications*, 2nd ed. John Wiley & Sons, Ltd, (2004).
- [17] M. R. Mohammad Younas, *Membrane Contactor Technology: Water Treatment, Food Processing, Gas Separation, and Carbon Capture*, 1st ed. Wiley-VCH, (2022).
- [18] A. Lee, J. W. Elam, and S. B. Darling, "Membrane materials for water purification: design, development, and application," *Environmental Science: Water Research & Technology*, 10.1039/C5EW00159E vol. 2, no. 1, pp. 17-42, (2016).
- [19] J. Jaafar and A. M. Nasir, "Grand Challenge in Membrane Fabrication: Membrane Science and Technology," (in English), *Frontiers in Membrane Science and Technology*, Specialty Grand Challenge vol. 1, 2022-April-13 (2022).

- [20] A. Bera, J. S. Trivedi, S. B. Kumar, A. K. S. Chandel, S. Haldar, and S. K. Jewrajka, "Anti-organic fouling and anti-biofouling poly (piperazineamide) thin film nanocomposite membranes for low pressure removal of heavy metal ions," *Journal of hazardous materials*, vol. 343, pp. 86-97, (2018).
- [21] J. E. Efome, D. Rana, T. Matsuura, and C. Q. Lan, "Insight studies on metal-organic framework nanofibrous membrane adsorption and activation for heavy metal ions removal from aqueous solution," *ACS applied materials & interfaces*, vol. 10, no. 22, pp. 18619-18629, (2018).
- [22] A. P. M. a. K. Oksman, "Materials and Energy: Handbook of Green Materials," (2014).
- [23] X. Dong, D. Lu, T. A. L. Harris, and I. C. Escobar, "Polymers and Solvents Used in Membrane Fabrication: A Review Focusing on Sustainable Membrane Development," *Membranes*, vol. 11, no. 5, p. 309, (2021).
- [24] V. L. Vilker, C. K. Colton, and K. A. Smith, "The osmotic pressure of concentrated protein solutions: effect of concentration and pH in saline solutions of bovine serum albumin," *Journal of Colloid and Interface Science*, vol. 79, no. 2, pp. 548-566, (1981).
- [25] L. Yang, Z. Shahrivari, P. K. T. Liu, M. Sahimi, and T. T. Tsotsis, "Removal of Trace Levels of Arsenic and Selenium from Aqueous Solutions by Calcined and Uncalcined Layered Double Hydroxides (LDH)," *Industrial & Engineering Chemistry Research*, vol. 44, no. 17, pp. 6804-6815, 2005/08/01 (2005), doi: 10.1021/ie049060u.
- [26] T. Paul and N. C. Saha, "Environmental Arsenic and Selenium Contamination and Approaches Towards Its Bioremediation Through the Exploration of Microbial Adaptations: A Review," *Pedosphere*, vol. 29, no. 5, pp. 554-568, 2019/10/01/ (2019).
- [27] S. Alka, S. Shahir, N. Ibrahim, M. J. Ndejiko, D.-V. N. Vo, and F. A. Manan, "Arsenic removal technologies and future trends: A mini review," *Journal of Cleaner Production*, vol. 278, p. 123805, 2021/01/01/ (2021).

- [28] T. Li *et al.*, "Treatment technologies for selenium contaminated water: A critical review," *Environmental Pollution*, vol. 299, p. 118858, 2022/04/15/ (2022).
- [29] A. O. Aguiar, L. H. Andrade, B. C. Ricci, W. L. Pires, G. A. Miranda, and M. C. S. Amaral, "Gold acid mine drainage treatment by membrane separation processes: An evaluation of the main operational conditions," *Separation and Purification Technology*, vol. 170, pp. 360-369, 2016/10/01/ (2016).
- [30] Y. He, J. Liu, G. Han, and T.-S. Chung, "Novel thin-film composite nanofiltration membranes consisting of a zwitterionic co-polymer for selenium and arsenic removal," *Journal of Membrane Science*, vol. 555, pp. 299-306, (2018).
- [31] Y. He, D. L. Zhao, and T.-S. Chung, "Na⁺ functionalized carbon quantum dot incorporated thin-film nanocomposite membranes for selenium and arsenic removal," *Journal of Membrane Science*, vol. 564, pp. 483-491, 2018/10/15/ (2018).
- [32] M. H. Zeeshan, R. U. Khan, M. Shafiq, and A. Sabir, "Polyamide intercalated nanofiltration membrane modified with biofunctionalized core shell composite for efficient removal of Arsenic and Selenium from wastewater," *Journal of Water Process Engineering*, vol. 34, p. 101175, 2020/04/01/ (2020).
- [33] F. H. Akhtar *et al.*, "Highways for water molecules: Interplay between nanostructure and water vapor transport in block copolymer membranes," *Journal of membrane science*, vol. 572, pp. 641-649, (2019).
- [34] G. Han, J. T. Liu, K. J. Lu, and T.-S. Chung, "Advanced Anti-Fouling Membranes for Osmotic Power Generation from Wastewater via Pressure Retarded Osmosis (PRO)," *Environmental Science & Technology*, vol. 52, no. 11, pp. 6686-6694, 2018/06/05 (2018).
- [35] Y. Lin *et al.*, "Zwitterionic Copolymer-Regulated Interfacial Polymerization for Highly Permselective Nanofiltration Membrane," *Nano Letters*, vol. 21, no. 15, pp. 6525-6532, 2021/08/11 (2021).
- [36] S. Bandehali, F. Parvizian, A. Moghadassi, and S. M. Hosseini, "High water permeable PEI nanofiltration membrane modified by L-cysteine functionalized

- POSS nanoparticles with promoted antifouling/separation performance," *Separation and Purification Technology*, vol. 237, p. 116361, 2020/04/15/ (2020).
- [37] S. Bandehali, A. Moghadassi, F. Parvizian, J. Shen, and S. M. Hosseini, "Glycidyl POSS-functionalized ZnO nanoparticles incorporated polyether-imide based nanofiltration membranes for heavy metal ions removal from water," *Korean Journal of Chemical Engineering*, vol. 37, no. 2, pp. 263-273, 2020/02/01 (2020).
- [38] J. D. Holmes, J. O'Connell, R. Duffy, and B. Long, "Surface Functionalization Strategies for Monolayer Doping," in *Encyclopedia of Interfacial Chemistry*, K. Wandelt Ed. Oxford: Elsevier, (2018)
- [39] S. Aryal. "NMR Spectroscopy- Definition, Principle, Steps, Parts, Uses." <https://microbenotes.com/nuclear-magnetic-resonance-nmr-spectroscopy/>.
- [40] A. Sarfraz, A. H. Raza, M. Mirzaeian, Q. Abbas, and R. Raza, "Electrode Materials for Fuel Cells," in *Encyclopedia of Smart Materials*, A.-G. Olabi Ed. Oxford: Elsevier, (2022), pp. 341-356.
- [41] "Radiological and Environmental Management." <https://www.purdue.edu/> .
- [42] B. Wang, X. Wu, T.-H. Gan, and A. Rusinek, "Finite element modelling of atomic force microscope cantilever beams with uncertainty in material and dimensional parameters," (2014).
- [43] H. Waheed and A. Hussain, "Preparation and solvents effect study of asymmetric cellulose acetated/polyethyleneimine blended membranes for dialysis application," *Int. J. Health Med.*, vol. 2, no. 4, pp. 5-9, (2017).
- [44] S. Filice *et al.*, "Applicability of a New Sulfonated Pentablock Copolymer Membrane and Modified Gas Diffusion Layers for Low-Cost Water Splitting Processes," *Energies*, vol. 12, no. 11, p. 2064, (2019).
- [45] H. Waheed, F. T. Minhas, and A. Hussain, "Cellulose acetate/sericin blend membranes for use in dialysis," *Polymer Bulletin*, vol. 75, no. 9, pp. 3935-3950, (2017).
- [46] N. Bhuchar, Z. Deng, K. Ishihara, and R. Narain, "Detailed study of the reversible addition–fragmentation chain transfer polymerization and co-polymerization of 2-

- methacryloyloxyethyl phosphorylcholine," *Polymer Chemistry*, 10.1039/C0PY00300J vol. 2, no. 3, pp. 632-639, (2011).
- [47] G. M. Shi, J. Zuo, S. H. Tang, S. Wei, and T. S. Chung, "Layer-by-layer (LbL) polyelectrolyte membrane with Nexar™ polymer as a polyanion for pervaporation dehydration of ethanol," *Separation and Purification Technology*, vol. 140, pp. 13-22, 2015/01/22/ (2015).
- [48] G. Han, S. S. Chan, and T.-S. Chung, "Forward Osmosis (FO) for Water Reclamation from Emulsified Oil/Water Solutions: Effects of Membrane and Emulsion Characteristics," *ACS Sustainable Chemistry & Engineering*, vol. 4, no. 9, pp. 5021-5032, 2016/09/06 (2016).
- [49] G. M. Nogueira *et al.*, "Preparation and characterization of ethanol-treated silk fibroin dense membranes for biomaterials application using waste silk fibers as raw material," *Bioresour Technol*, vol. 101, no. 21, pp. 8446-51, Nov (2010).
- [50] Z. Tan, S. Chen, X. Peng, L. Zhang, and C. Gao, "Polyamide membranes with nanoscale Turing structures for water purification," *Science*, vol. 360, no. 6388, pp. 518-521, (2018).